UNIVERSIDADE ESTADUAL DA PARAÍBA
PRÓ-REITORIA DE PÓS-GRADUAÇÃO E PESQUISA
PROGRAMA DE PÓS-GRADUAÇÃO EM ODONTOLOGIA
MESTRADO EM ODONTOLOGIA

ANA PRISCILA LIRA DE FARIAS FREITAS

AVALIAÇÃO DOS ARTEFATOS FORMADOS POR NÚCLEOS METÁLICOS FUNDIDOS: UM ESTUDO POR TCFC

CAMPINA GRANDE – PB
2017

ANA PRISCILA LIRA DE FARIAS FREITAS

AVALIAÇÃO DOS ARTEFATOS FORMADOS POR NÚCLEOS METÁLICOS FUNDIDOS: UM ESTUDO POR TCFC

Dissertação apresentada ao Programa de Pós-Graduação em Odontologia da Universidade Estadual da Paraíba-UEPB, em cumprimento às exigências para obtenção do título de Mestre em Odontologia.

Orientadora: Prof.ª Dr.ª Daniela Pita de Melo
Co-orientadora: Prof.ª Dr.ª Ana Marly Araújo Maia

CAMPINA GRANDE – PB

2017

F866a Freitas, Ana Priscila Lira de Farias.

Avaliação dos artefatos formados por núcleos metálicos fundidos [manuscrito] : Um estudo por TCFC / Ana Priscila Lira de Farias Freitas. - 2017

109 p. : il. colorido.

Digitado.

Dissertação (Mestrado em Odontologia) - Universidade Estadual da Paraíba, Centro de Ciências Biológicas e da Saúde, 2017.

"Orientação : Profa. Dra. Daniela Pita de Melo, Departamento de Odontologia - CCBS."

"Coorientação: Profa. Dra. Ana Marly Araújo Maia, Departamento de Odontologia - CCBS.""

1. Artefatos. 2. Metal. 3. Tomografia Computadorizada de Feixe Cônico. 4. Restaurações metálicas.

21. ed. CDD 617.6

ANA PRISCILA LIRA DE FARIAS FREITAS

AVALIAÇÃO DOS ARTEFATOS FORMADOS POR NÚCLEOS METÁLICOS FUNDIDOS: UM ESTUDO POR TCFC.

Dissertação apresentada ao Programa de Pós-Graduação em Odontologia da Universidade Estadual da Paraíba-UEPB, em cumprimento às exigências para obtenção do título de Mestre em Odontologia.

Aprovado em: 08/06/2017.

BANCA EXAMINADORA

____

Prof.ª Dr.ª Andrea dos Anjos Pontual de Andrade Lima – UFPE
MEMBRO TITULAR (EXAMINADORA EXTERNA)

____

Prof.ª Dr.ª Patrícia Meira Bento – UEPB
MEMBRO TITULAR (EXAMINADORA INTERNA)

____

Prof.ª Dr.ª Daniela Pita de Melo – UEPB
MEMBRO TITULAR (ORIENTADORA)

CAMPINA GRANDE – PB
2017

Dedico este trabalho:

A minha filha Ana Helena por ser minha fonte diária de energia.

AGRADECIMENTOS ESPECIAIS

A DEUS pela vida.

A minha mãe, Alcione, por todo o amor e dedicação a família e pelo constate incentivo e apoio ao estudo.

Ao meu pai, Antônio, por todo o amor e por sempe olhar dentro do meu olho e falar: “já deu certo!”

Aos meus irmãos pelo companheirismo e apoio. E em especial a minha irmã Alana, pelas incansáveis horas cuidando da minha filha para que eu pudesse estudar.

Ao meu marido, Thiago, pelo companheirismo e amor, pela paciência na compreensão dos momentos de ausência por conta dos estudos e pelo apoio na vida acadêmica.

A minha filha, Ana Helena, que recarrega minhas energias com seu maravilhoso sorriso e carinho!

A minha sogra, Dona Helena, pelo imenso amor a neta e por todos os dias que cuidou de Ana Helena.

Aos meus familiares e amigos, por todo apoio, e especial a minha prima Juliana.

Aos professores do Programa de Pós-Graduação em Odontologia, pelas valiosas contribuições científicas e ensinamentos.

À orientadora Profª. Drª Daniela Pita de Melo, pela graciosa condução da orientação. Sempre com um sorisso no rosto e com muita gargalhada mesmo diante das inesperadas surpresas e dificuldades que acompanham as pesquisas. Obrigada pelo carinho e pela confiança.

À minha co-orienradora Profª. Drª Ana Marly Araújo Maia, por todo o incentivo, carinho, paciência, dedicação e pelos ensinamentos!

À Profª. Drª Patrícia Meira Bento por sua dedicação a Pós-graduação e em especial pela oportunidade de realização da pesquisa na ABO.

À Profª. Ms Karla Rovaris Silva, por toda colaboração na pesquisa.

Ao Prof. Dr. Yuri Wanderley Cavalcanti, por sua paciência e contribuições e com a estatística do trabalho.

Ao Prof. Gustavo Godoy, pelo incentivo ao mestrado.

Aos colegas da turma de mestrado, pela convivência em alegria e pela ajuda mútua.

À minha amiga Luana, pelo companheirismo, pelas alegrias e dificuldades compartilhadas. É um anjinho em forma de uma linda mulher que ilumina a vida de todos! Obrigada por tudo!

À equipe de pesquisa de Radiologia, por transfomar a exaustão das pesquisas em momentos divertidos. Em especial a Larissa, Martina, Elisa e Fernanda pela agradável convivência e força durante a realização do trabalho.

À ABO e a UFPE, pelo acolhimento, especialmente nas figuras dos funcionários Ana e Sérgio.

Agradeço a todas as pessoas que diretamente ou indiretamente contribuíram para a realização dessa conquista.

‘’Não existe caminho para o conhecimento. O conhecimento é o caminho’’

Mahatma Gandhi

FREITAS, A. P. L. F. Avaliação dos artefatos formados por núcleos metálicos fundidos: um estudo por TCFC. 109f. il. 2017. Dissertação (Mestrado) – Departamento de Odontologia, Universidade Estadual da Paraíba, Campina Grande, 2017.

RESUMO

Este estudo teve como objetivo avaliar, qualitativamente e quantitativamente, os artefatos formados por dois tipos de núcleos metálicos fundidos por meio da Tomografia Computadorizada de feixe cônico (TCFC). Trata-se de um estudo experimental *in vitro*, com amostra composta por 20 pré-molares inferiores humanos, divididos em dois grupos: Grupo Ni-Cr - 10 dentes que receberam os núcleos de Níquel-Cromo; Grupo Ag-Pd – 10 dentes que receberam núcleos de Prata-Paládio; e por dois dentes extras (um de cada liga). As amostras foram preparadas com secção da coroa dentária, seguidas de instrumentação, obturação e desobturação das raízes, para moldagem e confecção do núcleo metálico em dimensões similares. Para o escaneamento as amostras foram posicionadas em um crânio seco dentado, recoberto com cera nº 7 e imerso em água para simular a condição clínica. Todos os dentes foram escaneados vazios, com os núcleos metálicos (condição intracanal) e em duas condições orais: 1) Simples - um dente da amostra e 2) Dupla - o dente da amostra e um dente extra. As amostras foram escaneadas usando o tomógrafo CS 9000 3D TCFC com dois parâmetros de exposição: 85kV 6,3mA e 85kV 10mA. A presença de artefato foi avaliada qualitativamente por dois observadores previamente calibrados (análise do volume e análise de imagem pareada – para halos hipodensos, linhas hipodensas e linhas hiperdensas). A análise quantitativa foi realizada por um observador treinado, utilizando o software ImageJ (National Institutes of Health, Bethesda, MD, EUA). Para análise qualitativa dos artefatos, os dados foram submetidos ao teste de Wilcoxon, teste de Kruskal-Wallis, Mann-Whitney e Qui quadrado. Para a análise quantitativa, utilizou-se ANOVA bidirecional, teste de Tukey e teste T pareado, com nível significativo de 5% ($p < 0,05$). Para a análise qualitativa do volume, observaram-se diferenças estatísticas significativas entre os metais estudados em condição oral dupla, maior para AgPd, para os halos e linhas ($p = 0,006$) e entre as duas condições orais ($p = 0,033$), maior para duplo, para linhas hipo e hiper. Para análise qualitativa das imagens pareadas, houve diferenças estatísticas significativas apenas entre as condições intracanais (maior para AgPd). Na análise quantitativa das imagens foi confirmada a presença de maior percentual de área acometida por artefatos no grupo AgPd ($p = 0.002$) e na condição oral dupla ($p<0.001$). Concluiu-se que os parâmetros de exposição testados não interferiram na quantidade de formação de artefatos. Ligas de números atômicos superiores geram maior quantidade de artefatos. Observou-se que a presença de outro metal nos maxilares, condição dupla, acentuou a intensidade dos artefatos.

Palavras-chave: Artefatos, Metal, Tomografia Computadorizada de Feixe Cônico.

FREITAS, A. P. L. F. Assessment of artifacts formed by metal posts: a CBCT study. 109p. Ill. 2017. Department of Dentistry, State University of Paraiba, 2017.

ABSTRACT

This study aimed to assess, subjectively and objectively, the image artifacts of two types of metal posts using Cone Beam Computed Tomography (CBCT). This *in-vitro* experimental study was composed of 20 inferior premolars, divided in two groups: Group Ni-Cr – 10 teeth that were casted with nickel-chromium posts; Group Ag-Pd – 10 teeth that were casted with silver-palladium posts; and two extra teeth (one from each alloy). The sample were prepared after the section of the dental crown, followed by instrumentation, obturation and root unblocking, for molding and confection of the metal. For image acquisition the samples were placed in a dry dentate skull, covered with wax n° 7 and immersed in water to simulate the clinical condition. The sample were scanned using CS 9000 3D CBCT scanner with two exposure parameters: 85kV 6,3mA and 85kV 10mA. All the teeth were scanned empty, with the metal posts (intracanal condition) and in two oral conditions: 1) Single - one test tooth and 2) Double- the test tooth and extra tooth. The presence of artifact was assessed qualitatively by two previously calibrated observers (volume analysis and paired image analysis - for hypodense halos, hypodense lines and hyperdense lines). Quantitative analysis was performed by one trained observer, using Image J (National Institutes of Health, Bethesda, MD, USA). For qualitative artifact analysis, data were submitted to Wilcoxon test, Kruskal-Wallis, Mann-Whitney and Qui square test. For quantitative analysis, 2-way ANOVA, Tukey test and paired T-test was used with the significant level set at 5% ($p<0.05$). For the qualitative analysis of the volume, significant statistical differences were observed between the metals studied in double oral condition, higher for AgPd, for halos and lines ($p = 0.006$) and between the two oral conditions ($p = 0.033$), higher for double, for hypo and hyper lines. For paired image quality analysis, there were significant statistical differences only between metal posts (higher for AgPd). For quantitative images analysis it was confirmed the presence of a higher percentage of area affected by artifacts in the AgPd ($p = 0.002$) group and in the double oral condition ($p<0.001$). It was concluded that the exposure parameters tested did not interfere in the amount of artifact formation. Higher atomic number alloys generate greater amount of image artifacts. It was observed that the presence of another metal, double condition, accentuated the intensity of the artifacts.

Key-words: Artifacts, Metals, Cone-Beam Computed Tomography.

LISTA DE ILUSTRAÇÕES

LISTA DE QUADROS

LISTA DE TABELAS

ARTIGO

LISTA DE ABREVIATURAS, SIGLAS E SÍMBOLOS

Ag	Prata
Al	Alumínio
Au	Ouro
Ba	Bário
BSE	*Backscattering electrons* (Elétrons retroespalhados)
CCTS	Centro de Ciências Tecnologia e Saúde
CEP	Comitê de Ética em Pesquisa
Cm	Centímetros
CMOS	Semicondutor de metal-óxido complementar (*Complementary metal-oxide-semiconductor*)
CNS	Conselho Nacional de Saúde
Cr	Cromo
CRT	Comprimento real de trabalho
Cu	Cobre
DICOM	*Digital Imaging and Communications in Medicine* (Imagem digital e comunicação em medicina)
EDTA	Ácido etileno diamino tetracético
FOV	Campo de visão (*Field of view*)
GIMP	GNU *Image Manipulation Program* (Programa de manipulação de imagem)
kV	Quilovoltagem
mA	Miliamperagem
MAR	*Metal artifact reduction* (Redução de artefato de metal)
MEV/EDS	Microscopia eletrônica de varredura/Espectrometria de energia dispersiva (*Energy Dispersive System*)
Mm	Milímetros
µm	Micrômetro
Mg	Magnésio
Mo	Molibidênio
Ni	Níquel

NIH	*National Institutes of Health* (Instituto Nacional de Saúde)
NiTi	Níquel-titânio
NMF	Núcleo metálico fundido
Pd	Paládio
SE	S*ecundary electrons* (Elétrons secundários)
Seg	Segundos
Si	Silício
TC	Tomografia computadorizada
TCFC	Tomografia computadorizada de feixe cônico
TCLE	Termo de consentimento livre e esclarecido
Ti	Titânio
UEPB	Universidade Estadual da Paraíba
UFPE	Universidade Federal de Pernambuco
Zn	Zinco
2D	Bidimensional
3D	Tridimensional
%	Por cento; percentual de
°	graus

SUMÁRIO

1 CONSIDERAÇÕES INICIAIS

A tomografia computadorizada de feixe cônico (TCFC) é o avanço tecnológico mais significativo nas imagens maxilofaciais desde a introdução da radiografia panorâmica, anunciando uma mudança na natureza bidimensional (2D) da imagem radiográfica para volumétrica (3D), produzindo imagens precisas e de qualidade para um diagnóstico apurado no campo da Odontologia (WHITE; PHAROAH, 2014; MORTMAN, 2011).

O advento da TCFC representou o desenvolvimento de um tomógrafo relativamente pequeno e de menor custo, especialmente indicado para a região dentomaxilofacial (GARIB et al., 2007). O aparelho utiliza uma fonte de radiação ionizante em forma de cone divergente e um detector fixo sobre um pórtico rotativo para fornecer múltiplas imagens sequenciais que são integradas diretamente, formando um volume de informações (WHITE; PHAROAH, 2014). Os tomógrafos realizam um giro parcial, total ou até dois giros ao redor do objeto a ser escaneado, utilizando em sua maioria, um feixe de raios X de forma pulsátil, que atravessa e é atenuado pelo objeto até ser captado pelos sensores (BELEDELLI; SOUZA, 2012).

1.1 TCFC E FORMAÇÃO DE ARTEFATOS

O desenvolvimento e rápida comercialização da tecnologia TCFC dedicada à imagem da região maxilofacial, vem aumentando consideravelmente o acesso dos profissionais à avaliação radiográfica volumétrica na clínica odontológica (SCARFE; FARMAN; SUKOVIC, 2006), apresentando indicações em diversas áreas da Odontologia, tais como a dentística, endodontia, periodontia, prótese, diagnóstico, cirúrgica, implante e ortodontia (KAMBUROGLU, 2015).

Um número crescente de dispositivos de TCFC tornaram-se disponíveis ao longo dos últimos anos, exibindo uma gama de aparelhos com variados parâmetros de exposição, tais como campo de visão (FOV), qualidade do feixe (pico de tensão e filtração), quantidade de raios X (corrente do ânodo e a exposição tempo), e do arco de rotação. Além disso, diferentes tamanhos e tipos de detectores são utilizados, e diferentes algoritmos de reconstrução são aplicados (PAUWELS et al., 2013).

Todos estes parâmetros podem influenciar no diagnóstico e na qualidade da imagem em termos de ruído, resolução, contraste e presença de artefatos (PAUWELS et al., 2013). Portanto, os operadores de unidades de TCFC devem seguir uma seleção cuidadosa dos protocolos de exposição, varredura e formatação de imagem para otimizar exibição de imagem e minimizar a dose de radiação do paciente (WHITE; PHAROAH, 2014).

Os sistemas geralmente geram as imagens no formato *Digital Imaging and Communications in Medicine* - DICOM (padrão internacional para imagens médicas), onde os volumes podem, portanto, ser exportados para qualquer outro software compatível com DICOM, assim como importar imagens de outros sistemas, simplificando a partilha de resultados. Podem também ser feitas capturas de tela que são facilmente transmitidas.

Em uma situação ideal, com alta dose de radiação, com muitos fótons, raios X monocromáticos, resolução de detector infinito, detectores perfeitos, nenhum movimento, e nenhuma dispersão, as imagens de tomografia computadorizada (TC) seriam um reflexo perfeito da realidade. Se qualquer uma dessas condições não forem satisfeitas, os artefatos estarão então presentes (BOAS; FLEISCHMANN, 2012).

De modo geral, um artefato de imagem pode ser definido como qualquer distorção ou erro na imagem que não está relacionada ao objeto em estudo, possivelmente induzidos por discrepâncias entre as reais condições físicas e a formatação matemática utilizada para fazer uma reconstrução em três dimensões (3D) (SCHULZE et al., 2011).

Tais problemas relacionados à qualidade das imagens tomográficas surgem conforme sua crescente aplicabilidade no dia a dia da prática odontológica. Os artefatos de imagem despontam como um dos maiores fatores de perda da qualidade de diagnóstico diante das imagens adquiridas nos tomógrafos de feixe cônico, podendo vir a prejudicar as imagens ao ponto de levar a um diagnóstico equivocado (BELEDELLI; SOUZA, 2012).

São vários os tipos de artefatos que podem estar presentes nas imagens tomográficas, como os de ruído, endurecimento do feixe, dispersão, espalhamento, movimento, anel e artefatos de metal, apresentando diversos fatores que determinam o seu aparecimento (BELEDELLI; SOUZA, 2012; BOAS; FLEISCHMANN, 2012; KUTEKEN et al., 2015).

Segundo Barret e Keat (2004) podem ocorrer os seguintes tipos de artefato: Estrias, geralmente devido a uma inconsistência em uma única medição do detector; Sombreamento, devido a um grupo de canais ou pontos de vista que divergem gradualmente da medida verdadeira; Artefato em anel, devido a erros na calibração de um detector individual e Distorção, devido à reconstrução helicoidal.

É possível agrupar as origens dos artefatos em quatro categorias (BARRET; KEAT, 2004): 1) Artefatos baseados na física, resultantes dos processos físicos envolvidos na aquisição de dados de TC; 2) Artefatos baseados no paciente, causados por fatores como o movimento do paciente ou a presença de materiais metálicos no paciente; 3) Artefatos gerados pelo tomógrafo, resultantes de imperfeições na função do tomógrafo; 4) Artefatos helicoidais e multi-slice, dependendo do método de reconstrução de imagem empregado.

Para evitar os artefatos de movimento derivados do paciente, o uso de auxiliares de posicionamento pode ser suficiente para prevenir o movimento voluntário na maioria dos pacientes. No caso de presença de metais, os pacientes são solicitados normalmente a retirar objetos metálicos removíveis, como jóias, antes de iniciar a aquisição da imagem. Mas alguns itens não são removíveis, como restaurações dentárias, próteses (coppings e núcleos metálicos fundidos), implantes, parafusos cirúrgicos (BARRET; KEAT, 2004).

A presença de corpos muito densos, como as diferentes ligas metálicas muito utilizadas nas diversas especialidades odontológicas, produz artefatos (SCARFE; FARMAN, 2008). Artefatos de metal encontrados em todos os tipos de tomografia computadorizada (SCHULZE et al., 2011), são causados por vários mecanismos de interação dos raios X com o metal, a depender do tipo e das bordas e extremidades do objeto. Dentre os artefatos resultantes dessa interação, ressaltam-se o endurecimento do feixe, beam starvation, os efeitos de dispersão e o ruído (BOAS, FLEISCHMANN, 2012).

O endurecimento do feixe ocorre quando se utiliza uma fonte de raios X policromáticos, os quais apenas fótons de raios X de alta energia passam através do metal, e os fótons de baixa energia serão atenuadas, de forma que a transmissão de raios X policromáticos vão seguir diferentes padrões de decaimento exponencial (PAUWELS et al., 2013; BOAS; FLEISCHMANN, 2012). O feixe resultante torna-se mais energético (sua energia média aumenta porque os fótons de menor energia são absorvidos), fazendo com que a imagem dos limites do objeto metálico tenha a aparência mais brilhante do que no centro. O resultado nas imagens são faixas claras e brilhantes, hiperdensas, que dificultam a visualização anatômica da região (KUTEKEN et al., 2015; BELEDELLI; SOUZA, 2012).

Outro tipo de artefato relativo ao endurecimento do feixe são manchas ou faixas escuras (hipodensas). Isso ocorre porque a porção do feixe de raios X que passa pelo centro dos objetos muito densos é atenuada abruptamente, diferente da porção do raio que passa na superfície, fazendo com que as áreas próximas a estruturas muito densas percam qualidade na formação da imagem (KUTEKEN et al., 2015; BELEDELLI; SOUZA, 2012). Essas interações são comumente observadas com os materiais com elevado número atômico, tais como osso, iodo, ou metal, que aumentam dramaticamente a atenuação do feixe, resultando em artefatos na imagem tomográficas (PAUWELS et al., 2013; BOAS; FLEISCHMANN, 2012).

Beam starvation ocorre devido à absorção completa do feixe pelo material e nenhuma exposição do sensor, que é codificado pelo *software* como uma linha brilhante (hiperdensa) (JAKOBSON et al., 2014, MOUDI et al., 2014).

A dispersão faz com que os fótons de raios X mudem a sua direção e energia, e assim, acabem em uma posição diferente no detector, que teriam poucos fótons. Em particular, blocos de metal dispersam todos os fótons, de forma que o detector correspondente irá detectar fótons espalhados ocupando posição diferente da real (BOAS; FLEISCHMANN, 2012).

O ruído ocorre devido a um erro estatístico de baixa contagem de fótons, e resulta em faixas aleatórias finas brilhantes e escuras que aparecem preferencialmente na direção de maior atenuação. Com um aumento de ruído, objetos de alto contraste como ossos podem ainda estar visíveis, mas os limites dos tecidos moles de baixo contraste podem ficar obscuros (BOAS; FLEISCHMANN, 2012).

O resultado dos artefatos de metal em imagens tomográficas linhas radiolúcidas e radiopacas e faixas radiolúcidas que dificultam a visualização anatômica da região, podendo até impossibilitar o diagnóstico em algumas áreas (SCARFE; FARMAN, 2008), como, por exemplo, a identificação de fraturas radiculares (MENEZES et al., 2016). Esses artefatos acontecem porque a densidade do metal está além da faixa normal que pode ser otimizada pelo computador (BARRET; KEAT, 2004).

Um bom design de tomógrafo minimiza alguns tipos de artefatos e alguns podem ser parcialmente corrigidos pelo software. Quando é impossível fazer a varredura da anatomia desejada sem incluir objetos metálicos, a formação de listras pode ser grandemente reduzida por meio de correções especiais de software. Os fabricantes usam uma variedade de técnicas de interpolação para substituir os valores de *over range* em perfis. A ferramenta de redução de artefatos metálicos de alguns aparelhos é por vezes limitada, porque, embora as listras distantes dos objetos metálicos sejam removidas, permanece ainda uma perda de detalhe em torno da interface metal/tecido, que é frequentemente a principal área de interesse do diagnóstico. No entanto, em muitos casos o posicionamento cuidadoso do paciente e a seleção precisa dos parâmetros de varredura são os fatores mais importantes para evitar a formação artefatos de imagem (BARRET; KEAT, 2004).

1.2 RESTAURAÇÕES METÁLICAS INTRARRADICULARES

As restaurações metálicas, as coroas, os suportes, os implantes, os núcleos metálicos fundidos (NMF), e vários outros metais utilizados na prática odontológica são exemplos de estruturas que podem afetar a qualidade de uma imagem tomográfica através dos artefatos produzidos (SCHULZE et al., 2011). Os efeitos resultam em diferentes tipos de deterioração da imagem, variando de riscos brilhantes que irradiam do metal, escurecimento de áreas na sua vizinhança e ainda a perda completa de valores de cinza entre objetos metálicos adjacentes. Como consequência, as regiões de interesse para o diagnóstico, planejamento ou acompanhamento não são corretamente visualizadas (PAUWELS et al., 2013).

Os núcleos metálicos fundidos, apesar de serem uma das mais antigas opções para restauração de dentes tratados endodonticamente, ainda continuam sendo muito empregados e proporcionam resultados clínicos satisfatórios (MORO; AGOSTINHO; MATSUMOTO, 2005), desde que indicados segundo variáveis como a posição que o dente ocupa no arco dentário, o tipo de oclusão do paciente, a forma anatômica do canal radicular, além da reabilitação protética como um todo.

A produção dos NMF, no laboratório de prótese, é realizada pela técnica direta de fundição da cera perdida. Um modelo de cera ou resina Duralay (padrão para fundição) é produzido na forma desejada e em de material resistente. É submetido a altas temperaturas, de forma que toda a resina seja derretida e removida pela queima, deixando uma cavidade na forma desejada. O espaço criado é então preenchido com a liga metálica derretida (fundida), de modo que o metal assuma a forma da escultura de resina original (NOORT, 2004).

Uma liga seria a combinação de um ou mais metais, ou com um ou mais não-metais. As ligas metálicas utilizadas para este fim são variadas, e a sua escolha é determinada por vários fatores, como o custo, biocompatibilidade, resistência a corrosão e ao embaçamento, dureza, entre outras características, que são consequências da constituição que apresentam (ANUSAVICE, 2005; NOORT, 2004). Atualmente as bases das ligas utilizadas nos NMF variam entre: ouro, paládio, prata, cobalto, níquel ou titânio e os elementos complementares são os mais variados.

As ligas de Níquel-Cromo são ligas de metais básicos (não-nobres) e amplamente utilizadas nos NMF. Apresentam o níquel como seu componente principal, além de 20% de cromo, 4% de molibidênio e 2% de berílio. São ligas muito duras, e embora de difícil polimento, a superfície final polida é resistente a arranhões e também a corrosão. As temperaturas de fusão variam de acordo com a composição, mas situam-se na faixa de 1200-1500 ºC, consideravelmente maior que as ligas de ouro (McCABE; WALLS, 2006).

As ligas de Prata-Paládio são brancas e predominantemente compostas de prata, mas com uma quantidade substancial de paládio (pelo menos 25%), que fornece nobreza e promove a resistência à corrosão e ajuda a impedir o embaçamento, que geralmente é associado à prata. Tais ligas foram introduzidas na década de 60 como uma alternativa às ligas de alto teor de ouro, porém elas ainda podem ou não conter uma pequena quantidade de ouro ou de cobre. As temperaturas de fundição estão na faixa das ligas amarelas de ouro (ANUSAVICE, 2005; NOORT, 2004).

Um dos problemas comumente associado aos núcleos metálicos é a possibilidade de induzirem à concentração de tensões no ápice radicular, por apresentarem módulo de elasticidade superior ao da dentina, quando da incidência de forças laterais no dente, podendo levar à fratura. Um problema clínico a longo prazo das raízes de dentes gravemente comprometidos tratados com NMFs é o elevado percentual de fraturas radiculares em curto e médio prazo (LOURO; VIERA; FIRME, 2008).

Diante do exposto, os artefatos de imagem ameaçam a qualidade diagnóstica das imagens geradas pelos tomógrafos e são alvo de estudos que pesquisam formas de eliminá-los ou pelo menos diminuí-los (PAUWELS et al., 2013; CODARI et al., 2017; BENIC et al., 2013; LIKUBO et al., 2016). Como sua intensidade pode ser influenciada pelo material, ou por características de escaneamento do tomógrafo, o presente estudo teve como objetivo avaliar a formação de artefatos formados por núcleos metálicos fundidos, comparando dois tipos de ligas metálicas, selecionados segundo composição química e número atômico, assim como comparar a influência de diferentes parâmetros de mA.

2 OBJETIVOS

2.1 OBJETIVO GERAL

O presente estudo se propõe a avaliar os artefatos formados por núcleos metálicos fundidos por meio da TCFC.

2.2 OBJETIVOS ESPECÍFICOS

- Avaliar qualitativamente e quantitativamente os tipos e intensidade dos artefatos formados pelo núcleo metálico fundido de Niquel-Cromo nas imagens de TCFC;
- Avaliar qualitativamente e quantitativamente os tipos e intensidade dos artefatos formados pelo núcleo metálico fundido de Prata-Paládio nas imagens do TCFC;
- Comparar qualitativamente e quantitativamente a intensidade dos artefatos segundo a variação de parâmetros;
- Comparar qualitativamente e quantitativamente a intensidade dos artefatos segundo a variação de material;
- Comparar qualitativamente e quantitativamente a intensidade dos artefatos segundo a variação de condição oral (simples ou duplo);
- Comparar quantitativamente a intensidade dos artefatos segundo os terços cervicais, médio e apicais do núcleo.

3 MATERIAIS E MÉTODOS

3.1 DELINEAMENTO DO ESTUDO

O estudo consistiu em uma pesquisa experimental *in vitro.*

3.2 LOCAL DO ESTUDO

A pesquisa foi realizada nos Laboratórios de Prótese Dentária e Endodontia do Departamento de Odontologia da Universidade Estadual da Paraíba – UEPB para procedimentos de preparo da amostra.

Para aquisição das imagens, a pesquisa foi desenvolvida em dois locais: 1) Associação Brasileira de Odontologia – Seção PB, João Pessoa – Paraíba, onde foram realizadas as tomografias; 2) Laboratório de Microscopia Eletrônica da Universidade Federal de Pernambuco, Recife – Pernambuco, para realização da Microscopia eletrônica de varredura/Espectrometria de energia dispersiva (MEV/EDS).

3.3 ASPECTOS ÉTICOS

O projeto foi cadastrado na Plataforma Brasil (ANEXO A) e submetido ao Comitê de Ética em Pesquisa (CEP) da Universidade Estadual da Paraíba com aprovação sob o número CAAE: 60637616.6.0000.5187 (ANEXO B). A pesquisa seguiu a resolução 466/12 do Conselho Nacional de Saúde (CNS) e está em conformidade com a Declaração de Helsinque.

O Termo de doação de dentes (ANEXO C) foi assinado pelo dentista que realizou as exodontias. Uma vez que não é possível identificar os indivíduos doadores dos dentes, sujeitos da pesquisa, não será aplicado o termo de consentimento livre e esclarecido (TCLE) (APÊNDICE A).

O Termo de retirada do crânio e da mandúbula do Laboraório de Morfofisiologia do Curso de Odontologia do CAMPUS VIII/UEPB foi assinado pelo diretor do Centro de Ciências, Tecnologia e Saúde-CCTS UEPB (ANEXO D).

3.4 AMOSTRA

Foram selecionados 20 pré-molares inferiores unirradiculares para a amostra e 2 dentes extras, segundo observação dos critérios de inclusão e exclusão na análise de radiografias periapicais digitais, utilizando-se o aparelho de raios X Expert DC (Gendex® Dental System, Itália) e as placas de armazenamento de fósforo número 2 do sistema radiográfico digital Digora Optime® (Milwaukee, WI, EUA), com 70 kV, 7 mA, tempo de exposição de 0,13 segundos e distância foco-filme de 32 cm. Todos os dentes foram inspeccionados por transiluminação para verificar a ausência de fraturas radiculares.

Como critério de inclusão foram aceitos os dentes com raízes completamente formadas, dimensões semelhantes, canal radicular único e relativamente reto (inclinação máxima da raiz de $\leq 5°$ de acordo com o método de Schneider - 1971).

Como critério de exclusão foi considerada a presença de nódulos pulpares, reabsorção interna e/ou externa, tratamento endodôntico prévio, multiplicidade de canais, obliteração de canal, fratura de raiz e anomalias.

3.5 CARACTERIZAÇÃO DA AMOSTRA

Os 20 pré-molares foram divididos, aleatoriamente, em dois grupos experimentais, cada qual com dez dentes (n=10) segundo a liga metálica do núcleo metálico fundido, sendo eles:

Grupo Ni-Cr: Dentes que receberam núcleo metálico fundido de Níquel-Cromo;

Grupo Ag-Pd: Dentes que receberam núcleo metálico fundido de Prata-Paládio.

3.6 PREPARO DAS AMOSTRAS

Os dentes pertencentes à amostra foram submetidos a raspagem radicular e alisamento da superfície, com auxílio de cureta periodontal (Trinity Odontologia, São Paulo, SP, Brasil). Em seguida, foram esterilizados em autoclave (M9UltraClave Dabi Atlante, Ribeirão Preto, SP, Brasil) e imersos em solução salina de NaCl 0,9% (ADV, Nova Odessa, São Paulo, Brasil).

Os espécimes selecionados tiveram sua porção coronária removida por meio de um corte perpendicular ao longo eixo da raiz, na altura da junção amelocementária com auxílio de um disco diamantado (KG Sorensen, Zenith Dental ApS, Agerskov, Dinamarca) e micromotor elétrico (LB 100, Beltec, Araraquara, SP, Brasil). Em seguida os dentes foram inseridos separadamente em tubos de polipropileno tipo Eppendorf (Micro Test Tubes 3810X standard - Eppendorf do Brasil Ltda, São Paulo, SP, Brasil), com solução salina (NaCl 0,9% - ADV, Nova Odessa, São Paulo, Brasil), identificados numericamente (Figura 1) e dispostos em um suporte, facilitando sua localização.

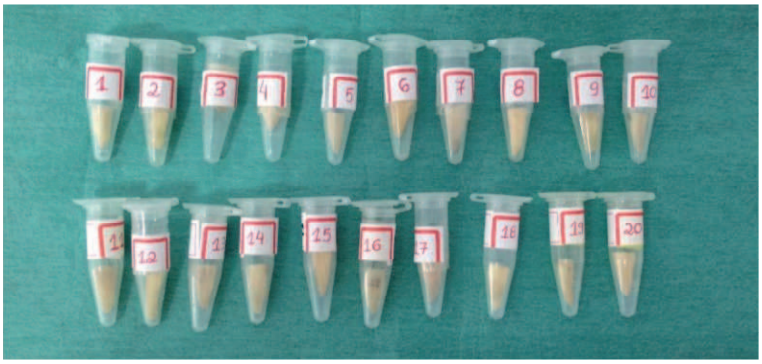

Figura 1. Dentes nos Eppendorfs identificados numericamente.
FONTE: Pesquisador.

3.6.1 Preparo do canal radicular

Os dentes tiveram o canal radicular irrigado com 2ml de hipoclorito de sódio a 2,5% (Ciclo farma, Serrana, SP, Brasil) (Figura 2) com auxílio de uma seringa para irrigação (Ultradent Products Inc., South Jordan, UT, EUA) e agulha Endo-Enze (Ultradent Products Inc., South Jordan, UT, EUA). Os dentes foram instrumentados com o sistema Reciproc R50

(VDW, Munique, Alemanha) (Figura 3). O diâmetro final do conduto correspondeu a 1/3 do diâmetro da raiz, o que foi respeitado até a última etapa para efeitos de comparação de áreas (Figura 4).

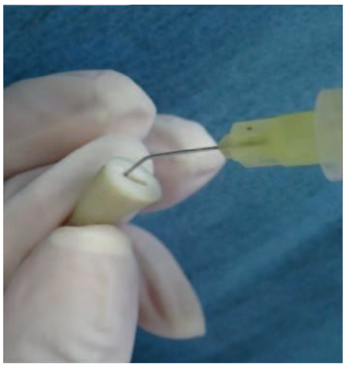

Figura 2. Irrigação com 2ml de hipoclorito de sódio a 2,5%.
FONTE: Pesquisador.

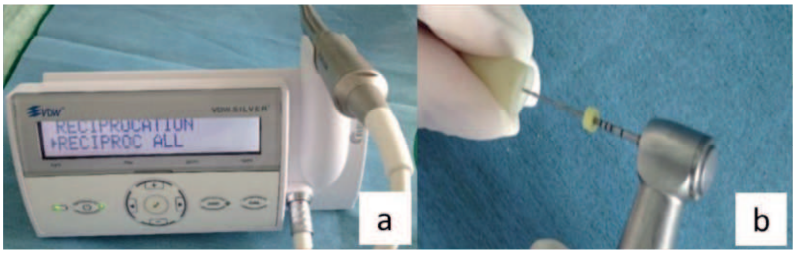

Figura 3. Instrumentação com sistema Reciproc R50. Motor (a). Posicionamento da lima (b).
FONTE: Pesquisador.

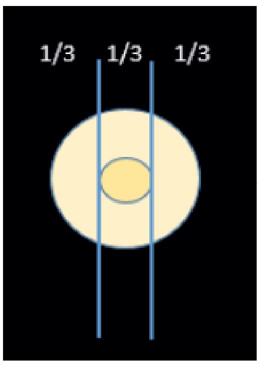

Figura 4. Proporções entre o conduto e a dentina.
FONTE: Pesquisador.

Finalizada a instrumentação, os condutos radiculares passaram por uma irrigação final com 2ml de ácido etileno diamino tetracético (EDTA) a 17% (Biodinâmica Química e Farmacêutica Ltda, Ibiporã, PR, Brasil) (Figura 5), por 3 min sendo agitado com o auxílio de uma lima manual tipo k 15.

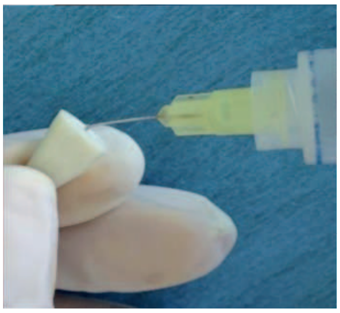

Figura 5. Irrigação 2ml de EDTA a 17%.
FONTE: Pesquisador.

3.6.2 Obturação dos canais radiculares

Após a instrumentação do canal radicular, os dentes foram obturados pela técnica de Compactação Termomecânica. Para isso foram utilizados cones de papel absorvente do sistema Reciproc (VDW, Munique, Alemanha) que possuíam a mesma conicidade dos instrumentos utilizados (Figura 6), além do cimento Sealer 26 (Dentsply, Rio de Janeiro, Brasil), com sua manipulação seguindo as recomendações do fabricante.

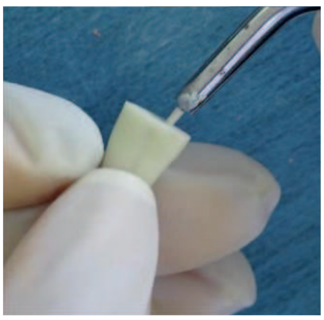

Figura 6. Cones de papel absorvente para secar o canal.
FONTE: Pesquisador.

Esta técnica de Compactação Termomecânica foi executada através da adaptação de um cone de guta-percha (Reciproc R50, VDW, München, Alemanha) de tamanho e conicidade idênticos ao instrumento utilizado no preparo mecânico (Figura 7a), seguida de pincelamento do cimento nas paredes do conduto e inserção do cone no comprimento real de trabalho (CRT) (Figuras 7b e c).

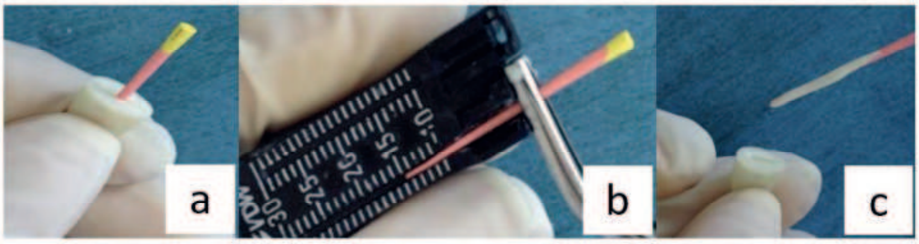

Figura 7. Obturação. Adaptação do cone de guta percha (a). Inserção do cone com cimento no CRT (b e c).
FONTE: Pesquisador.

O termocompactador PacMac 45.04 de 21 mm (SybronEndo Dental Specialties, Glendora, CA, EUA), montado em contra-ângulo com rotação para a direita, foi inserido ao lado do cone (Figura 8a). Quando acionado, em movimentos de bicada, o instrumento gerou fricção, amoleceu a guta-percha e a impulsionou apicalmente. A massa plástica foi compactada verticalmente com calcador frio (Figura 8b).

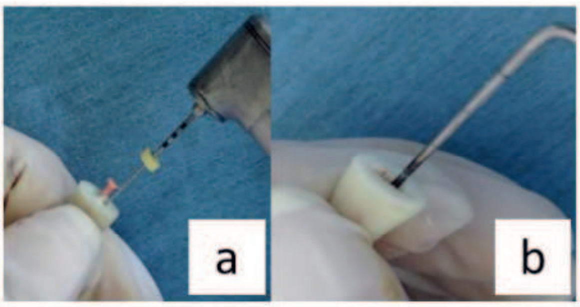

Figura 8. Termocompactação. Inserção da PacMac ao lado do cone (a). Compactação vertical (b).
FONTE: Pesquisador.

3.6.3 Ligas metálicas e caracterização por MEV/EDS

Foram escolhidas duas ligas com metais de número atômico diferentes e que são utilizadas na confecção de NMFs na prática clínica. Os elementos e suas porcentagens foram identificadas nas tabelas dos fabricantes e avaliadas por meio da Microscopia eletrônica de varredura e Espectrometria de energia dispersiva (MEV/EDS).

Para o Grupo Ni-Cr foram confeccionados núcleos metálicos de Niquel-Cromo com a liga fabricada e distribuída pela Talmax Produtos de Prótese Dentária Ltda (Curitiba, PR, Brasil), FIT CAST-SB Plus. O quadro 1 mostra as porcentagens dos elementos informadas pelo fabricante e as encontradas pelo MEV/EDS e a figura 9 mostra o mapeamento da liga pelo MEV/EDS (Figura 9).

Quadro 1. Composição da liga Níquel-Cromo.

COMPOSIÇÃO DA LIGA NÍQUEL-CROMO			FABRICANTE	MEV/EDS
DESCRIÇÃO	SÍMBOLO	NÚMERO ATÔMICO	%	%
Níquel	Ni	28	60,75%	62,3%
Cromo	Cr	24	25%	12,4%
Molibidênio	Mo	42	10%	4,1%
Silício	Si	14	2%	4,1%
Titânio	Ti	81	< 1%	*

* Elementos com porcentagens menor que 1% não são identificadas pelo MEV/EDS.

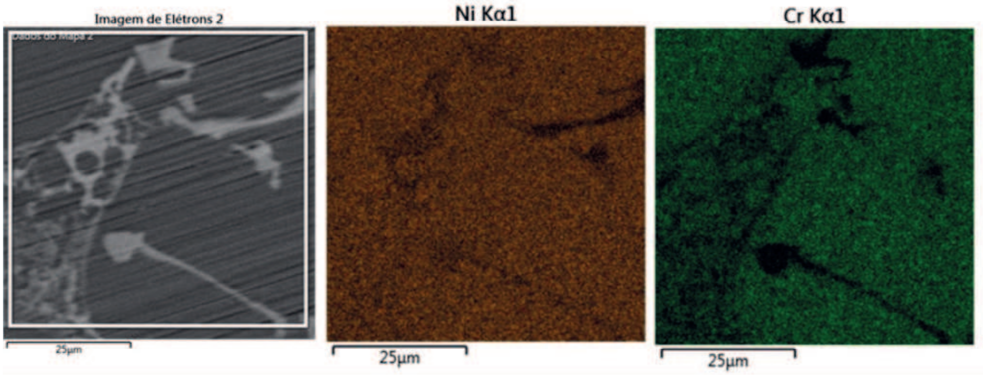

Figura 9. Mapeamento do NiCr pelo MEV/EDS.

Para o Grupo Ag-Pd foram confeccionados núcleos metálicos de Prata–Paládio com a liga da La Croix Ligas Dentais (Rio de Janeiro, RJ, Brasil), PALAD PD-AG (LPD). A composição fornecida pelo fabricante e as encontradas pelo MEV/EDS estão indicadas no quadro 2. A figura 10 mostra o mapeamento da liga de AgPd.

Quadro 2. Composição da liga Prata-Paládio.

COMPOSIÇÃO DA LIGA PRATA-PALÁDIO			FABRICANTE	MEV/EDS
DESCRIÇÃO	SÍMBOLO	NÚMERO ATÔMICO	%	%
Ouro	Au	79	7%	1,5%
Paládio	Pd	46	25%	22%
Prata	Ag	47	60%	64,4%
Cobre e outros	Cu	29	8%	11,3%

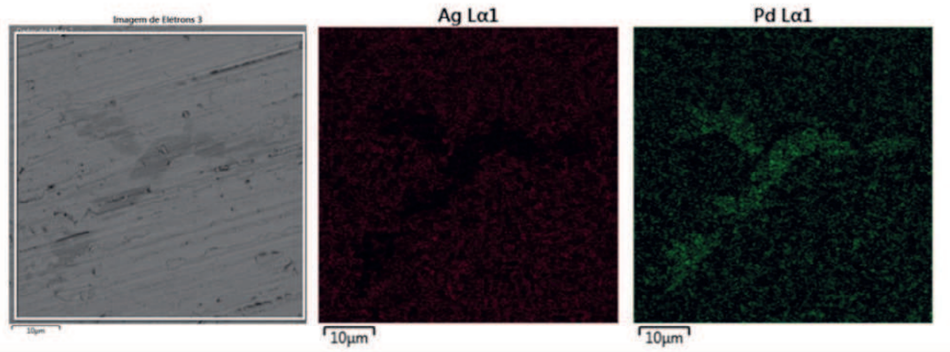

Figura 10. Mapeamento do AgPd pelo MEV/EDS.

3.6.4 Confecção dos núcleos metálicos fundidos

A confecção dos núcleos metálicos foi realizada pela técnica direta, que consiste na cópia idêntica da anatomia interna do conduto radicular. Inicialmente, foram desobturados 2/3 do comprimento do canal obturado (Broca Largo Peeso nº 1 e nº 2, DENTSPLY/MAILLEFER, Brasil), observados através de uma radiografia periapical (Figuras 11a e b). Com o limite adequado, o núcleo foi confeccionado em resina acrílica (Duralay) (Reliance Dental 13 Co, Worth, EUA), padrão para fundição (Figura 12), para a moldagem do conduto e enviado ao laboratório protético para fundição (Figuras 13a e b). A parte coronária do NMF foi padronizada com o uso de uma matriz de silicona de condensação, base pesada, (Zetaplus, Zhermack, Itália) (Figuras 14a e b), para que núcleos maiores ou menores não viessem a interferir na quantidade de artefato.

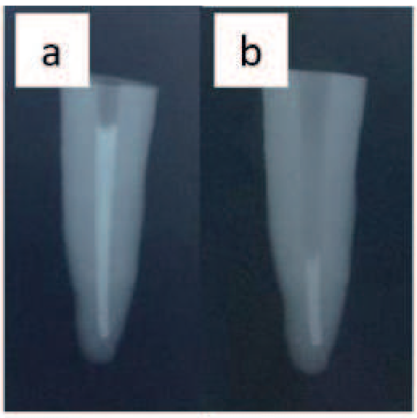

Figura 11. Radiografias. Obturação (a). Desobturação (b).
FONTE: Pesquisador.

Figura 12. Padrão para fundição em resina acrílica Duralay.
FONTE: Pesquisador.

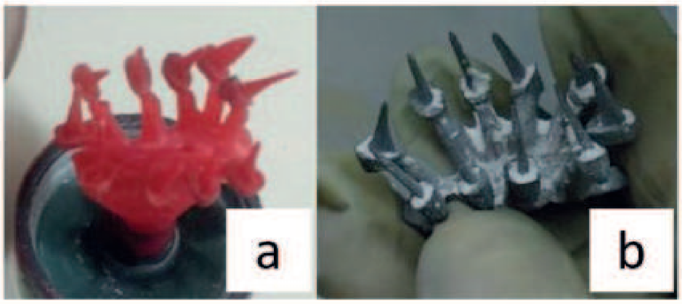

Figura 13. Fundição NMF. Inicial (a). Final (b).
FONTE: Pesquisador.

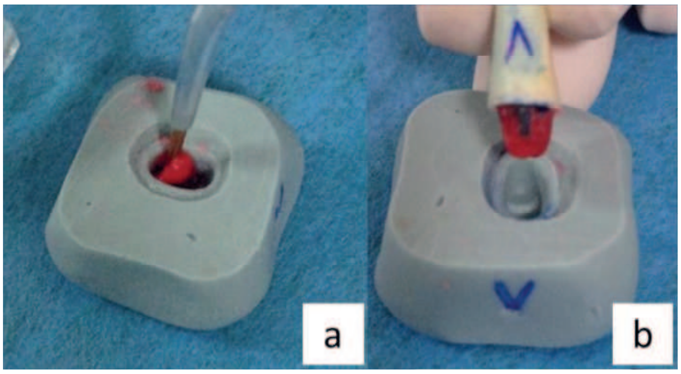

Figura 14. Matriz de Silicona de condensação. Inserção da resina (a). Remoção do conjunto/aspecto final (b).
FONTE: Pesquisador.

Após a adaptação e instalação dos núcleos, com auxílio da base leve da silicona de condensação (Oranwash/Indurent, Zhermack, Itália) (Figuras 15a, b e c), uma radiografia periapical foi realizada para avaliar a adaptação do núcleo metálico no canal radicular (Figura 16). As figuras 17 e 18 mostram todos os núcleos da amostra confeccionados.

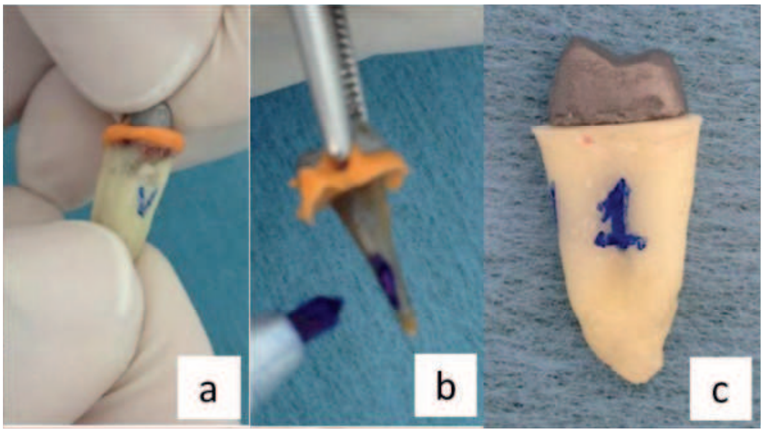

Figura 15. Adaptação do NMF. Moldagem com silicona leve (a). Adaptação final (b).
FONTE: Pesquisador.

Figura 16. Rx para verificar a adaptação do NMF.
FONTE: Pesquisador.

Figura 17. Núcleos MF de NiCr.
FONTE: Pesquisador.

Figura 18. Núcleos MF de AgPd.
FONTE: Pesquisador.

3.7 PREPARO DO CRÂNIO E MANDÍBULA

Para simular a interferência dos tecidos moles na formação da imagem a amostra foi posicionada em um crânio e mandíbula. Os mesmos foram recobertos com uma camada de 5 mm de espessura de cera rosa nº 7 (Figuras 19a, b, c e d e 20 a e b). Os dentes foram posicionados no alvéolo do canino inferior direito envoltos por uma fina camada de cera rosa nº 7. O conjunto crânio/mandíbula foi colocado numa caixa de isopor retangular contendo água para simular uma situação clínica (Figura 20c). Outros dentes (sem restaurações metálicas) foram posicionados nos alvéolos inicialmente vazios para simular a arcada de um paciente dentado (Figura 20d) (adaptado de PINTO et al., 2016).

Apesar da amostra ser toda representada por pré-molares, o alvéolo do canino foi o que conseguiu receber os dentes de forma que todos pudessem ficar posicionados no nível da base do osso alveolar (Figuras 21a, b e c).

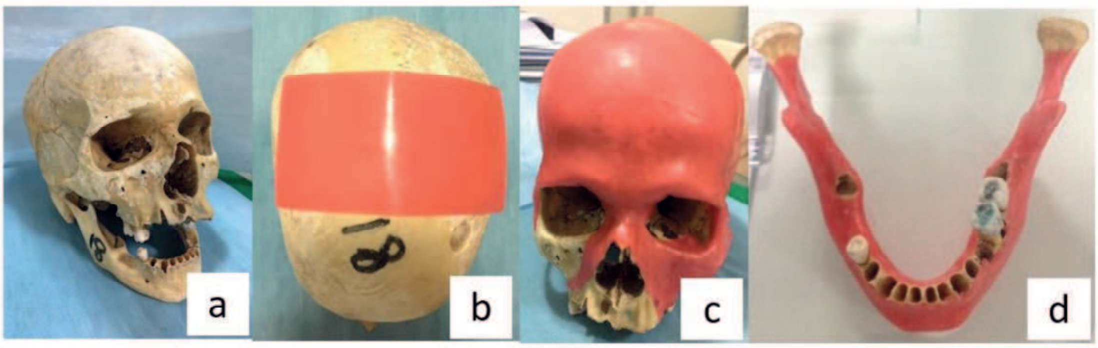

Figura 19. Recobrimento do crânio (a, b, c) e mandíbula (d) com cera.
FONTE: Pesquisador.

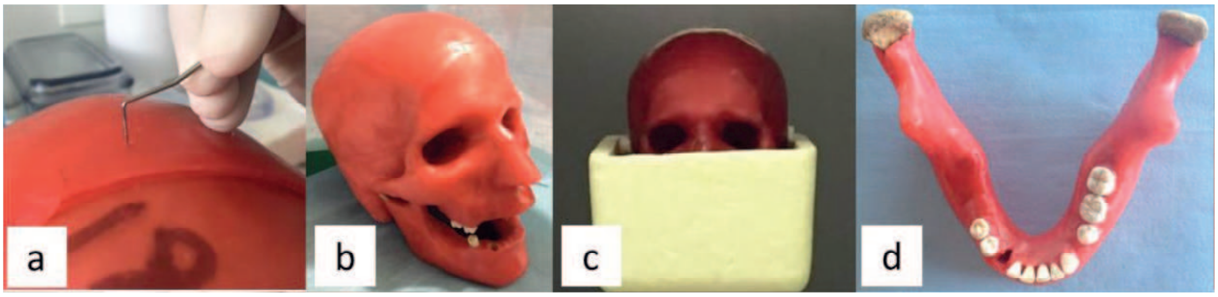

Figuras 20. Camada de 5mm de espessura de cera (a) e o aspecto final (b). Conjunto crânio/mandíbula dentro da caixa de isopor com água (c). Aspecto final da mandíbula dentada (d).
FONTE: Pesquisador.

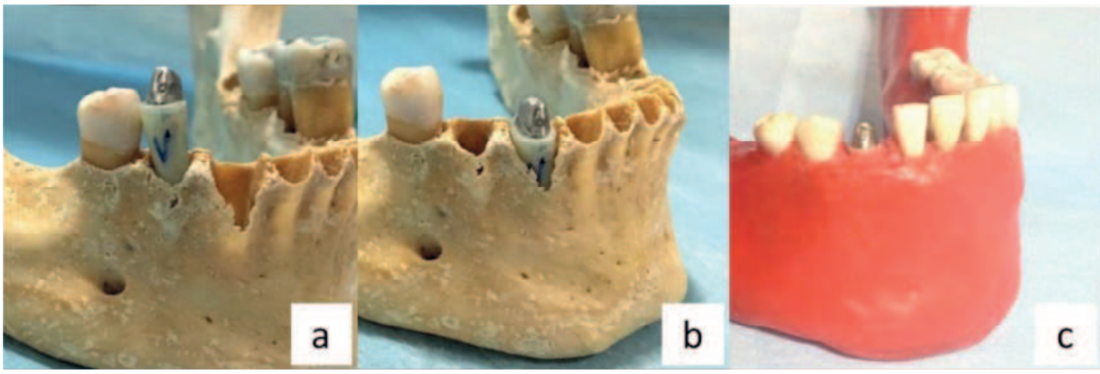

Figuras 21. Escolha do alvéolo para inserção da amostra. Alvéolo do pré-molar (a) e alvéolo do canino (b e c).
FONTE: Pesquisador.

3.8 AQUISIÇÃO DAS IMAGENS

As tomografias de feixe cônico foram adquiridas utilizando o aparelho KODAK CS 9000 3D (Carestream Dental) que apresenta um feixe cônico com sensor CMOS de fibra óptica, escala de cinza de 16 bits, campo de visão fixo de 5cm x 3,75cm, voltagem do tubo de 60-90 kV, corrente do tubo de 2-15 mA, voxel de 76, 100 ou 200 µm e o tempo de reconstrução de imagem de aproximadamente 2 minutos. Os escanementos foram realizados mantendo um tamanho de voxel de 0,100 mm, e o tempo de exposição foi de 10,80 segundos (Figura 22).

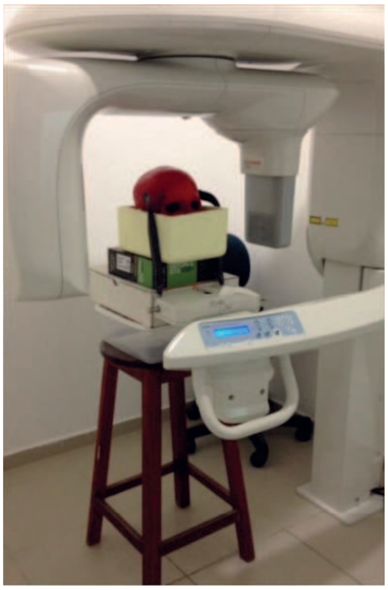

Figura 22. Escaneamento no tomógrafo Carestream (KODAK CS 9000).
FONTE: Pesquisador.

O escaneamento foi realizado em duas condições orais estabelecidas e denominadas de simples e duplo, vazio e passivo (adaptado), utilizando dois protocolos de exposição - 85 kV/6,3 mA 85 kV/10 mA, de acordo com a descrição na figura 23.

Figura 23. Descrição das condições de escaneamento.
FONTE: Pesquisador.

As imagens tomográficas foram salvas em formato DICOM para posterior visualização nos programas próprios do sistema utilizado (CS 3D Imaging Software - Carestream Dental Rochester, NY, EUA).

3.9 TREINAMENTO E CALIBRAÇÃO

Para as análises qualitativas dois observadores foram previamente calibrados utilizando CS 3D Imaging Software (programas de visualização do sistema tomográfico). O coeficiente Kappa inter-observador foi de 0.400 para halos hipodensos, 1.000 para linhas hipodensas e 0.700 para linhas hiperdensas O coeficiente de Kappa intraobservador, para o observador 1, foi de 1.000 para halos hipodensos, 0.700 para linhas hipodensas e hiperdensas. O coeficiente de Kappa intraobservador, para o observador 2, foi de 0.550 para halos hipodensos, 0.625 para linhas hipodensas e 0.550 para linhas hiperdensas. As análises quantitativas foram realizadas por um único observador, utilizando a ferramenta threshold do programa ImageJ (National Institutes of Health, Bethesda, MD, USA, http:// rsb.info.nih.gov/ij/).

3.10 ANÁLISE DAS IMAGENS

3.10.1 Análise Qualitativa

Para análise qualitativa volumétriva, dois radiologistas (orais e maxilofaciais) com um mínimo de 6 anos de experiência em análise tridimensional de imagens, treinados e calibrados, realizaram individualmente a análise qualitativa para avaliar o padrão de artefato das imagens. Os observadores receberam instruções verbais, práticas e escritas. Os ajustes de zoom, brilho e configurações de contraste foram deixados a critério de cada observador.

As imagens foram fornecidas sem dados de identificação e em ordem aleatória gravadas em HD externo (Samsung Modelo HX-M500TCB/G 500GB). Os volumes foram visualizados usando CS 3D Imaging Software (v3.1.9, Carestream Dental Rochester, NY, EUA) (Figura 24), exibidas no monitor a cores Ultra fina da DELL de 24 polegadas (Dell Inc, Austin, EUA) em uma sala silenciosa com luz esmaecida. Os observadores poderiam percorrer o volume tomográfico em todos os sentidos para avaliação dos artefatos. Foi sugerido uma quantidade diária de 15 volumes para avaliação com intervalo mínimo de 24h, porém cada avaliador ficou à vontade para escolher seu limite, não ultrapassando 50 imagens no dia, levando aproximadamente 1 mês para finalizar as avaliações.

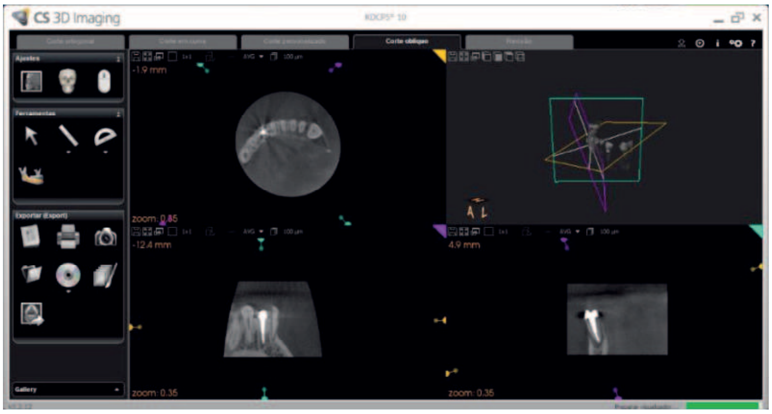

Figura 24. CS 3D Imaging Software.

Os observadores recebiam um informativo com orientações sobre a avaliação e quadros para preenchimento da escolha das intensidades dos artefatos (ANEXO E). Os Artefatos dos núcleos metálicos foram classificados usando uma adaptação de Vasconcelos et al. (2014): Ausência (0), presença moderada (1) e presença severa (2) para halo hipodenso (bandas escuras), linhas finas hipodensas (linhas escuras) e as linhas hiperdensas (raias) (Quadro 3). As imagens dos dentes vazios também foram classificadas como grupo de controle devido aos possíveis efeitos dos diferentes parâmetros a serem estudados na formação de artefato.

Quadro 3. Classificação e escores da avaliação subjetiva de artefatos.

Volume_____X_____	**Halo Hipodenso**	**Linhas Hipodensas**	**Linhas Hiperdensas**
Ausência (0)			
Presença moderada (1)			
Presença severa (2)			

Uma outra análise qualitativa foi a denominada análise qualitativa pareada, realizada pelos mesmos avaliadores, cegos quanto a condição simples ou duplo. Desta forma, ao invés do volume tomográfico, foram fornecidos uma combinação de dois volumes sempre em três cortes nos eixos coronal, sagital e axial (na mesma altura). Todos os cortes foram limitados a uma área de 6,00x4,47 cm, conforme figura 25.

As imagens foram fornecidas em pares, numeradas de 1 a 96 no formato tiff (cada figura com dois volumes), gravadas em HD externo (Samsung Modelo HX-M500TCB/G 500GB). Os avaliadores utilizaram o programa Image J (National Institutes of Health, Bethesda, MD, USA, http:// rsb.info.nih.gov/ij/) para visualizar as imagens. Foram selecionadas 32 figuras/pares para cada um dos seguintes questionamentos: quanto ao parâmetro, a condição intracanal (material) e a condição oral.

Os três cortes de um volume (coronal, sagital e axial) eram posicionados ao lado dos três cortes de outro volume a ser comparado. Para o parâmetro, todas as situações eram equivalentes, variando apenas o parâmetro 6,3 e 10 mA (Figura 25a). Para o material, a variação era observada entre as ligas NiCr e AgPd (Figura 25b). Quanto a condição oral, diferença apenas entre simples e duplo (Figura 25c).

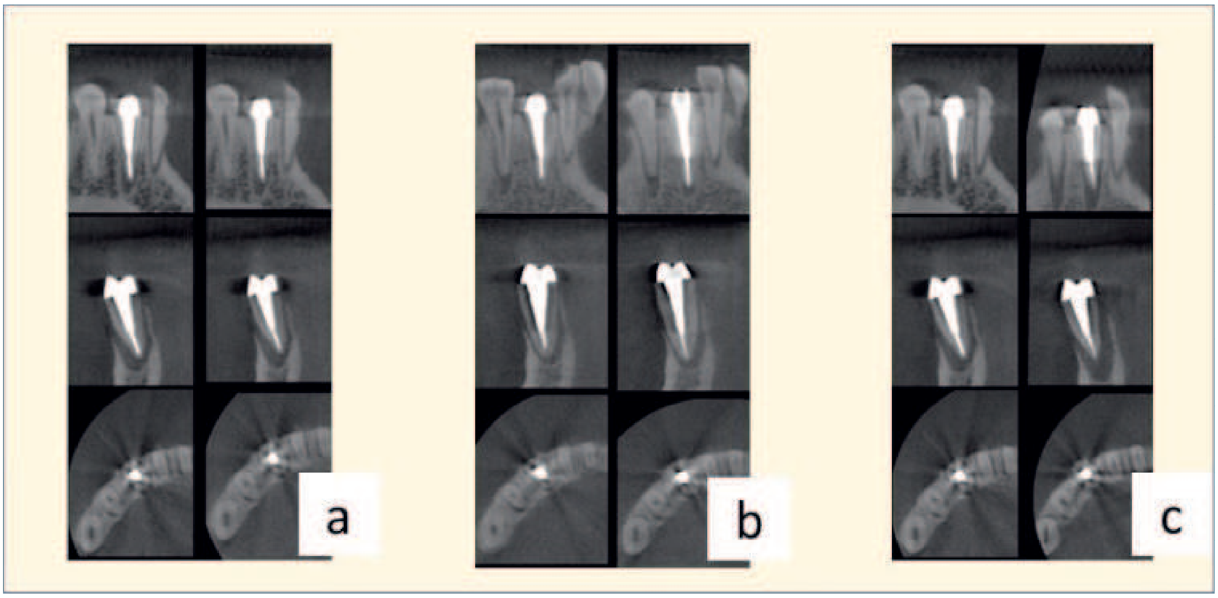

Figura 25. Figuras pareadas. Parâmetro (a). Material (b). Condição oral (c).
FONTE: Pesquisador.

Os avaliadores receberam um informativo com orientações sobre a avaliação e quadros para preenchimento da escolha de qual imagem apresentava maior quantidade de artefato: direita, esquerda ou não existia diferença (para os halos hipodenos, linhas hipodensas e linhas hiperdensas). Outro questionamento foi relacionado a questão de qualidade para diagnóstico. Qual das imagens apresenta maior qualidade para diagnóstico de fratura radicular? Direita, Esquerda ou não existia diferença (ANEXO F).

3.10.2 Análise Quantitativa

De modo quantitativo, a presença dos artefatos foi mensurada através do programa livre ImageJ, de acesso aberto, versão 1.41 (desenvolvido pelo *National Institute sof Health* (NIH), Bethesda, MD, EUA, http: // rsb.info.nih.gov/ ij /), que dispõe de ferramentas que possibilitam o uso de filtros, parâmetros de segmentação e realização de mensurações.

Cada arquivo DICOM (dentes vazios e com o núcleo passivo) foi lido no software nativo do scanner e três fatias axiais da raiz foram selecionadas e exportadas como uma imagem de Tiff. As fatias representavam o terço cervical, médio e apical do núcleo, sendo selecionadas a 2, 4 e 6 mm, respectivamente, da junção amelocementária (onde foi feito o corte para separar a coroa da raiz) (Figura 26).

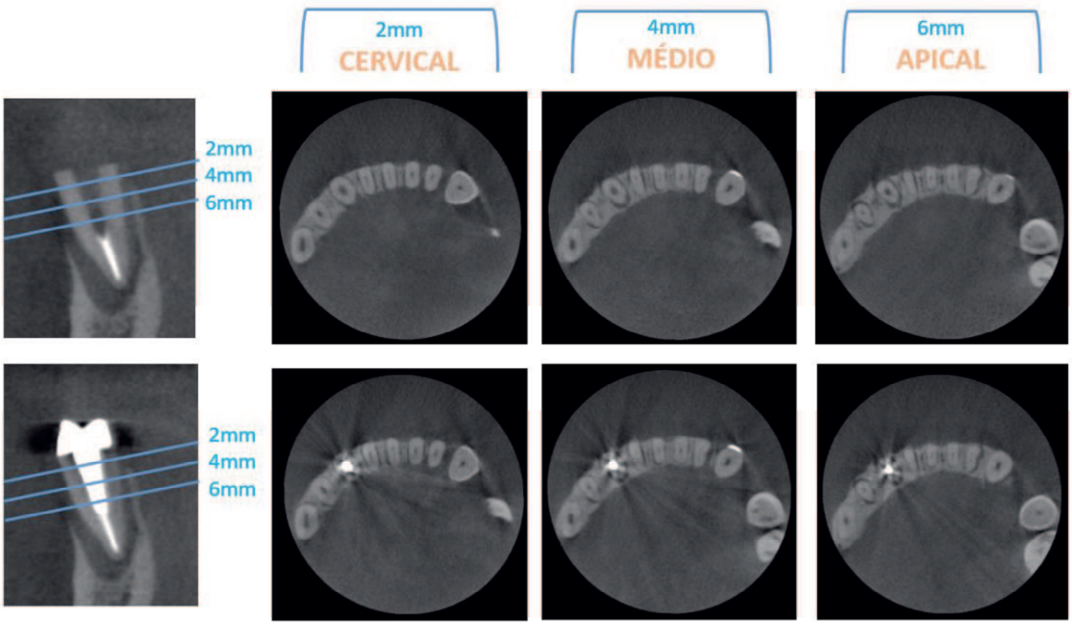

Figura 26. Fatias selecionadas (terço cervical, médio e apical do núcleo).
FONTE: Pesquisador.

As imagens axiais eram importadas no software GNU Image Manipulation Program (GIMP) (versão 2.8.14. A Equipe GIMP, EUA, disponível em: *http://www.gimp.org/*) e a região correspondente a toda área de raiz foi selecionada com a ferramenta de seleção livre visualizadas com um zoom de 200x (Figura 27a). As imagens resultantes foram fixadas em escala de 8 bits (256 níveis de cinza), salvas com um fundo preto no formato JPEG (Figura 26) e importados para ImageJ (Figura 27b).

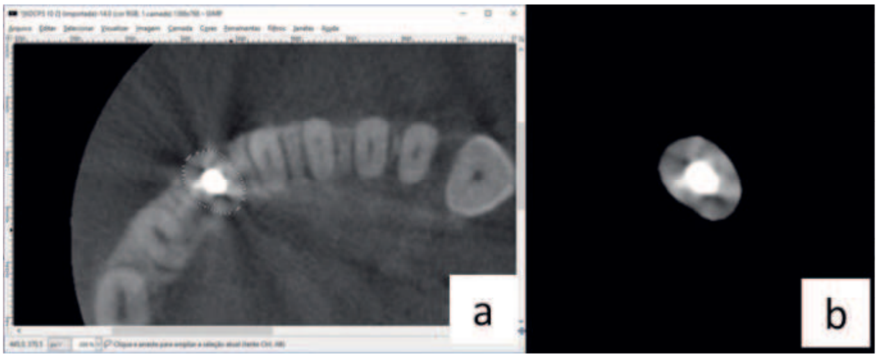

Figura 27. Seleção da área de raiz no programa GIMP (a). Área selecionada da raiz (b)
FONTE: Pesquisador.

Para remoção da área correspondente ao núcleo nas imagens com o núcleo passivo, que no caso não correspondem ao artefato de imagem, foi feita uma sobreposição entre as imagens do dente vazio e do dente com o núcleo passivamente adaptado. Esse processamento foi realizado no programa imageJ, nos três terços (cervical, médio e apical do núcleo) para a aquisição de uma imagem final de cada fatia axial (Figura 28).

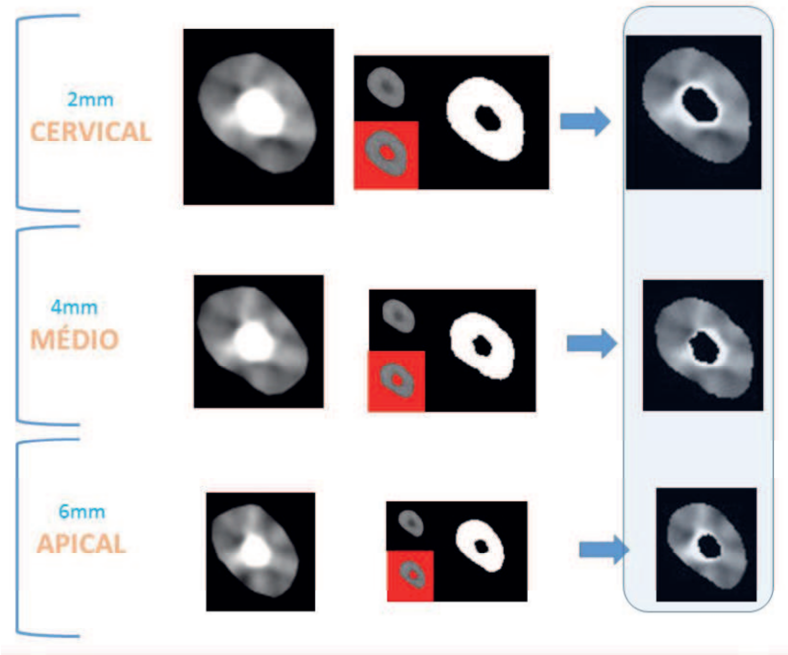

Figura 28. Processamento entre a imagem do dente com o núcleo e a imagem do dente vazio.
FONTE: Pesquisador.

Para o processamento das imagens, a imagem do dente vazio foi duplicada e foi aplicado a ferramenta Threshold de forma a selecionar o conduto vazio juntamente com o background (região preta). Com a imagem estabelecida, foi aplicado um binário, isto é, determinou que a parte selecionada ficasse correspondente a 0 (Zero) e a parte livre no caso dentina, seja igual a 255. Para possibilitar o processo, o binário deve ficar como zero e 1, logo foi feita a subtração de 254. A área do núcleo e background ficou correspondente a 0 e a dentina a 1. Foi feito então o processamento do cálculo da imagem, que no programa é uma multiplicação, do binário que tem o conduto vazio e dentina com a imagem com o núcleo e dentina. Como resultado, a parte da imagem correspondente ao núcleo foi excluída da imagem final.

A ferramenta Threshold do ImageJ também foi usada para determinar as áreas hipodensas de artefatos de imagem num limite de acordo com os valores de pixel da imagem avaliados (um range mínimo de 9 e máximo de 134 tons) (Figura 29a). Os mesmos passos foram utilizados para quantificação dos artefatos hiperdensos (limiar dos artefatos hiperdensos, com range mínimo de 147 e máximo de 255 tons) (Figura 29c). O remanescente de dente (dente não afetado) foi o range complementar entre o artefato hipo e o hiper (mínimo de 87 e máximo de 207) (Figura 29b).

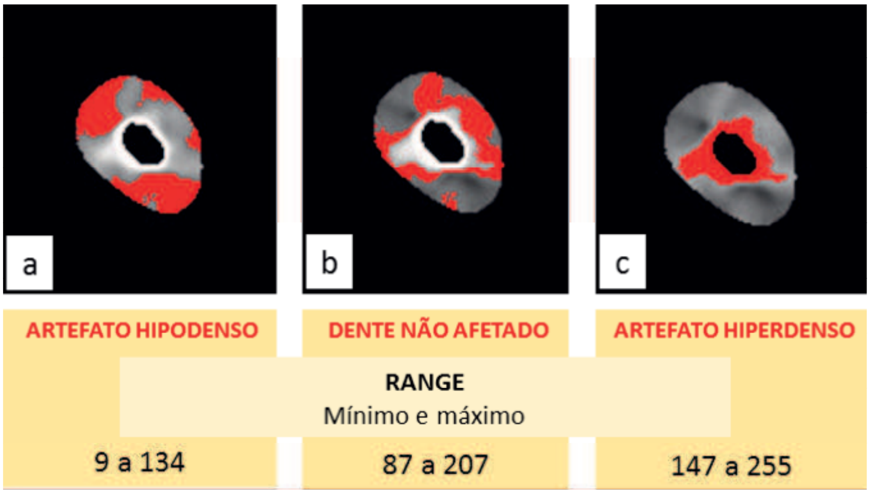

Figura 29. Seleção da área correspondente aos artefatos com a ferramenta Threshold. Hipodenso (a). Dente não afetado (b). Hiperdenso (c).
FONTE: Pesquisador.

Foram obtidas as áreas correspondentes ao artefato hipodenso, ao artefato hiperdenso e a área de dente não afetado. Em seguida, as porcentagens dessas áreas foram calculadas com base em cada valor de área dividido pela soma de todas as áreas.

3.11 ANÁLISE ESTÁTÍSTICA

Os dados foram tabulados e analisados estatisticamente no programa *Statistical Package for Social Sciences* (SPSS, v. 20, IBM, Chicago, IL). Todas as análises foram conduzidas considerando-se o nível de confiança de 95% (α<0,05). Inicialmente, os dados foram avaliados quanto a sua normalidade e heterogeneidade por meio do teste de Kolmogorov-Smirnov.

Para a análise qualitativa de artefatos, os dados foram submetidos ao teste de Wilcoxon para comparações estatísticas entre condições orais e testes de Kruskal-Wallis e Mann-Whitney para condições de enchimento intracanal e parâmetros de exposição TCFC. O teste do Qui quadrado foi utilizado para determinar desacordos entre os observadores durante a avaliação da qualidade da imagem pareada.

Para a análise quantitativa, a hipótese de diferença que avaliou o impacto dos parâmetros de TCFC e dos materiais envolvidos na construção NMFs foi avaliada por meio de Análise de Variância a dois fatores (ANOVA 2-way). Comparações pós-hoc foram avaliados pelo teste de

Tukey, quando a variável independente apresentou mais de 3 grupos. A hipótese de diferença que avaliou a o efeito dos dois modelos de estudo (simples e duplo) foi avaliada pelo teste t pareado.

4 RESULTADOS

Como se optou pela apresentação da dissertação em forma de artigo, os resultados serão descritos conforme a apresentação do artigo (Dentomaxillofacial Radiology).

5 ARTIGO

ARTIGO

Research article

ASSESSMENT OF METAL INTRACANAL POSTS ARTIFACTS:

A CONE-BEAM COMPUTED TOMOGRAPHY STUDY

Shortened version of the title: ARTIFACTS FORMED BY METAL POSTS

Ana Priscila Lira de Farias Freitas; Department of Oral Diagnosis, State University of Paraíba, Campina Grande – PB, Brazil;

Yuri Wanderley Cavalcanti; Department of Clinical and Social Dentistry, Federal University of Paraíba, João Pessoa, Brazil.

Patrícia Meira Bento; Department of Oral Diagnosis, State University of Paraíba, Campina Grande – PB, Brazil;

Ana Marly Araújo Maia; Department of Oral Diagnosis, State University of Paraíba, Campina Grande-PB, Brazil.

Karla Rovaris Silva; Department of Oral Diagnosis, State University of Paraíba, Campina Grande – PB, Brazil;

Daniela Pita de Melo; Department of Oral Diagnosis, State University of Paraíba, Campina Grande-PB, Brazil.

Correspondence Author:

Daniela Pita de Melo,

Rua Baraúnas, 351 - Bairro Universitário Campina Grande-PB, CEP 58429-500

Fax: +55 83 3315 3300.

E-mail: danipita@gmail.com

Date of Submission: xxxxxxx

ABSTRACT

Objectives: This study aimed to evaluate the intensity of two metal posts artifacts scanned using different exposure parameters and conditions. Material and Methods: The sample was composed of 20 inferior premolars, divided in two groups: Group Ni-Cr posts; Group Ag-Pd silver-palladium posts; and two extra teeth. All teeth were scanned with and without metal posts and in two oral conditions: 1) Single - one test tooth and 2) Double- the test tooth and a extra tooth. The samples were scanned using CS 9000 3D scanner with two exposure parameters: 85kV 6,3mA e 85Kv 10mA. The presence of artifact was assessed qualitatively by two calibrated observers, and quantitatively by one trained observer, using Image J. All analyzes were conducted considering the 95% confidence level ($\alpha < 0.05$). Results**:** For the qualitative analysis of the volume, statistical differences were observed between the metals studied in double oral condition, higher for AgPd, for halos and lines ($p = 0.006$) and between the two oral conditions ($p = 0.033$), higher for double, for hypo and hyper lines. For paired quality analysis, there were statistical differences only between intracanal conditions (higher for AgPd). For quantitative analysis it was confirmed the higher presence of artifact in the AgPd group and in the double oral condition. Conclusion: The exposure parameters tested did not interfere in the amount of artifact formation. Higher atomic number alloys generate greater amount of artifacts. The presence of another metal can increase the amount of artifact formation and impair CBCT diagnostic quality.

Keywords: Artifacts, Metals, Cone-Beam Computed Tomography.

INTRODUCTION

The introduction of cone-beam computed tomography (CBCT) for the maxillofacial region provides opportunities for dental practitioners to request multiplanar imaging[1] with enough quality and precision to establish an accurate diagnosis for all fields of dentistry.[2]

The number of CBCT devices available over the past few years has grown, exhibiting a range of devices with varying exposure parameters such as field of view (FOV), beam quality (peak voltage and filtration), amount of X-rays (anode current and time exposure), and the degrees of rotation. In addition, different sizes and types of detectors are used, and different reconstruction algorithms are applied in CBCT images.[2] All these parameters can influence the diagnosis and image quality in terms of noise, resolution, contrast and presence of artifacts.[2] Therefore, CBCT units' operators should carefully select the exposure, scanning and image formatting protocols to optimize image display and minimize patient radiation dose.[3]

The difficulties related to the quality of the tomographic images arise according to their increasing applicability in the dental practice. Image artifacts appear to be one of the major factors of impairment of the diagnostic quality of CBCT images.[4] In general, an image artifact can be defined as any distortion or error in the image that is unrelated to the object being studied, possibly induced by discrepancies between the actual physical conditions and the mathematical formatting used to make a reconstruction in three dimensions (3D).[5]

High-density materials are one of the main causes of artifacts, such as metal implants, intracanal posts, metallic crowns and amalgam restoration.[6] Metal artifacts are found in all types of computed tomography images acquired for dental purposes;[5] and are caused by several mechanisms, some of which are related to the type of metal alloy, others to the borders and different shapes of metal structures. The metal structures cause beam hardening, beam starvation, the effects of dispersion and noise.[7] Beam hardening is due to an unintentional attenuation of the x-ray beam by the material. The resultant beam becomes more energetic, resulting in darker lines. The latter is due to complete absorption of the beam by the material and no exposure of the sensor, which is coded by the software as a bright line.[8,9]

The resultant image of the metal artifacts in tomographic images are hypodense and hyperdense bands and lines that hinder the anatomical visualization of the region of interest and may even make diagnosis impossible in some cases,[10] such as identification of root fractures.[11,12,13] Metal posts (MP), despite being one of the oldest options for restoration of endodontically treated teeth, are still widely used and provide satisfactory clinical results.[14] One of the problems that are commonly associated to MP is the possibility of inducing concentration of tensions at the root apex, due to their modulus of elasticity which is superior to the dentin's modulus. When lateral forces are induced to the tooth, it can lead to root fracture. A clinical problem of severely teeth treated with MPs is the high percentage of root fractures in short and medium terms[15] and the difficulty of diagnosing these fractures.

Image artifacts are the subject of previous studies that investigated ways to quantify, eliminate or at least reduce them in tomographic images.[2,6,16,17] As its intensity may be influenced by the material, or by scanning characteristics of the CBCT scanner, the present study's objective is to evaluate, subjectively and objectively, the type and intensity of two molten metal posts artifacts scanned using different exposure parameters and conditions.

MATERIAL AND METHODS

This study consisted of an in vitro experimental research and was approved by State University of Paraíba Ethics and Research Committee (nº 39088714.2.0000.5187), and it is in compliance with Helsinki Declaration. Twenty single-rooted human teeth (premolars) extracted for therapeutic reasons, were included in the sample. Inclusion criteria determined that all teeth should present maximum root inclination of ≤5° according to Schneider's[18] method, and similar dimensions. All teeth were inspected by transillumination for the absence of root fractures and radiographed on phosphor plates (Digora Optime, Soredex, Tuusula, Finland) to exclude those teeth with pulp nodules, internal and/or external root resorption, previous endodontic treatment, root canal multiplicity root canal obliteration, root fractures, or any other anomaly.

Sample Preparation

After cleaning and disinfection protocols, teeth crowns were removed at the cemento-enamel junction and root canals were standardized using the Reciproc R50 system (VDW, München, Germany), thermomechanical compression filling then prepared to two thirds of the root length (Peeso Long Drill nº 1 and nº 2, DENTSPLY/MAILLEFER, Brasil) for posterior MP preparation and fitting.

The sample was divided into two groups: 10 teeth that received the nickel-chromium posts (NiCr group); 10 teeth that received the silver-palladium posts (AgPd Group).

The preparation of the MPs was performed by direct technique (standard for metal casting made of Duralay acrylic resin) and the coronary part of the MP was standardized using a heavy-base condensation silicone matrix (Zetaplus, Zhermack, Italy), so its size would not interfere in the number of artifacts present in the final CBCT image.

The FIT CAST-SB Plus alloy (Talmax Produtos de Prótese Dentária Ltda, Curitiba, PR, Brazil), was used to cast NiCr post group. For the Ag-Pd post Group the PALAD PD-AG (LPD) alloy (La Croix Dentales, Rio de Janeiro, RJ, Brazil) was used. All cast metal posts were passively fit and non-cemented. Periapical radiographs were taken to validate the MPs adaptations. Scanning electron microscopy/Energy Dispersive System (MEV/EDS) identified chemical composition, their percentages and distribution in the NiCr and AgPd alloys to validate the composition stated by the alloys' fabricants.

For scanning procedures, a dentate dry human skull was coated with a 5-mm-thick piece of wax to simulate the interference of soft tissues in the image. Each tooth was coated with a 0.2 mm layer of wax to be placed in an empty mandible right canine socket. The skull was immersed in a foam box filled with water to also simulate soft tissue coverage (adapted from Pinto[12]).

Image Acquisition

Each sample was scanned empty and with their corresponding MPs (NiCr or AgPd). The empty sample volumes were acquired as references for evaluation of the inference of artifacts in the MP CBCT volumes. CBCT scans were acquired using CS 9000 3D unit (Carestream Dental Rochester, NY, USA). Two sets of CBCT scans were obtained varying tube current - 6,3 mA and 10 mA. Voxel size, field of view (FOV) and tube voltage were fixed at 0.100 mm, 5 cm x 3.75 cm and 85kV, respectively, for all scans.

The CBCT scans were acquired also comparing two oral conditions: 1) Single – with a test tooth placed in the mandible socket of the canine and 2) Double- with a test tooth placed in the mandible socket of the canine and a non-test tooth with a passively fit MP placed in the opposite mandible canine socket. The MP of the non-test tooth was always the same material used to cast the test tooth.

A total of 160 volumes were acquired (twenty teeth test teeth, empty and with MPs, in two different tube currents and two different oral conditions). The resulting dataset was exported as DICOM files and saved with a code corresponding to the tooth, study groups, study conditions, and parameter protocol used.

Artifact Qualitative Analysis

Prior to all examination sessions, verbal and practical instructions and calibration tests were performed. Two oral and maxillofacial radiologists with a minimum of 6 years of experience in tridimensional image analysis evaluated all images independently. Adjustments on zoom, brightness and contrast settings were left to each observer's discretion. For the qualitative analysis volumes, the Kappa inter-observer coefficient was 0.400 for hypodense halos, 1.000 for hypodense lines and 0.700 for hyperdense lines. The Kappa intra-observer coefficient, for observer 1, was 1.000 for hypodense halos, 0,700 for hypodense and hyperdense lines. The Kappa intra-observer coefficient, for observer 2, was 0.550 for hypodense halos, 0.625 for hypodense lines and 0.550 for hyperdense lines. For paired image qualitative analysis, the kappa for parameter was 0.812 for hypodense halos and lines and 0.531 for hyperdense lines. For material was 0.437 for hypodense halos, 0.719 for hypodense lines and 0.906 for hyperdense lines. For condition was 0.719 for hypodense halos, 0.906 for hypodense lines and 0.719 for hyperdense lines.

Two qualitative analysis were performed. The first analysis was done assessing the CBCT volumes one per time; and the second one was done pairing the slices of the anatomical planes (coronal, sagittal and axial) of two different tested situations to allow blind evaluation and to minimize any possible induction in the evaluator's responses by the presence of the extra metal post on the other side of the arch in the double oral condition situations.

Qualitative analysis of the CBCT volumes

The scans were supplied in random order in a hard-drive (HD Samsung Model HX-M500TCB/G 500GB). The volumes were visualized using CS 3D Imaging Software (Carestream Dental Rochester, NY, USA) (Figure 1), displayed on a 24-inch DELL Ultra Sharp Color Monitor (Dell Inc, Austin, USA) in a quiet, dimly lit room. The observers evaluated the whole volume fore artifacts. A daily amount of 15 volumes was suggested for evaluation with a minimum interval of 24h, but each evaluator could choose his limit as long as it did not exceed 50 volumes per day.

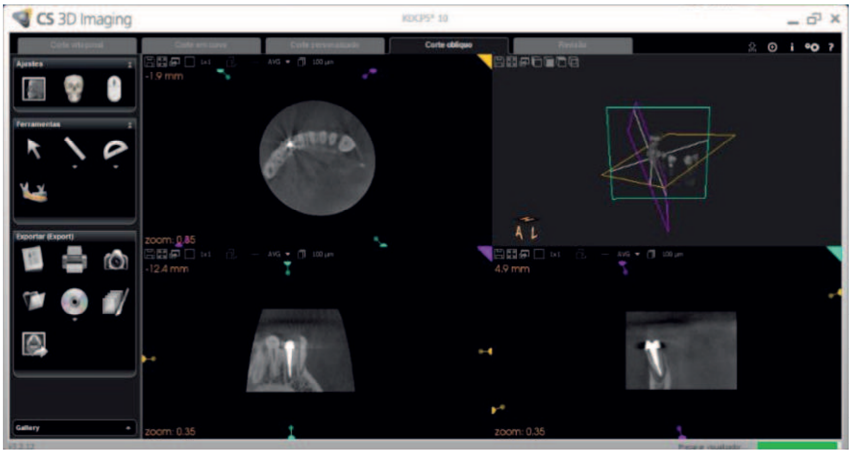

Figure 1. CS 3D Imaging Software.

The amount of image artifact was scored using an adaptation of Vasconcelos et al. (2014): Absence (0), moderate presence (1) high presence (2) for hypodense halo (dark bands), hypodense lines (dark lines) and hyperdense lines (bright lines). The images of the empty teeth were also classified as a control group due to the possible effects of the different tested parameters on artifact formation.

Paired image qualitative analysis

For the paired image qualitative analysis, the observers received coronal, sagittal and axial slices of one the test teeth paired with the anatomical plane slices of a second test tooth. Each DICOM file was read on the scanner's native software (CS3D imaging software, v3.1.9. Carestream Dental Inc., Rochester, USA) and three anatomical planes (axial, coronal and sagittal) slices of the root were selected and exported as a DICOM image. Datasets in compressed DICOM format were uncompressed with CS3D imaging software tool. All slices were limited to an area of 6.00x4.47cm. All slices were obtained in the same anatomical plane level as the first set of images.

The images were provided to the observers in pairs, numbered from 1 to 96, in tiff format (each set of figures with two different study samples), in a hard drive HD (Samsung Model HX-M500TCB/G 500GB). The observers used the Image J program (National Institutes of Health, Bethesda, MD, USA, http: // rsb.info.nih.gov/ij/) to view the images, displayed in a 24 inch color monitor (Ultra Sharp, Dell Inc., Austin, TX, USA), placed in a quiet room with dimmed light.

The images were paired to evaluate qualitatively the influence of the studied mA, MPs and oral conditions (single or double) by visual judgment of two experienced radiologists. To allow statistical comparison, 32 pairs of each tested variable were provided to each observer. For all groups of paired images, all variables were fixed and only the tested variable for that group varied, i.e.: for exposure parameter evaluation, all the other aspects of image acquisition were fixed, except for mA (6.3 and 10) (Figure 2).

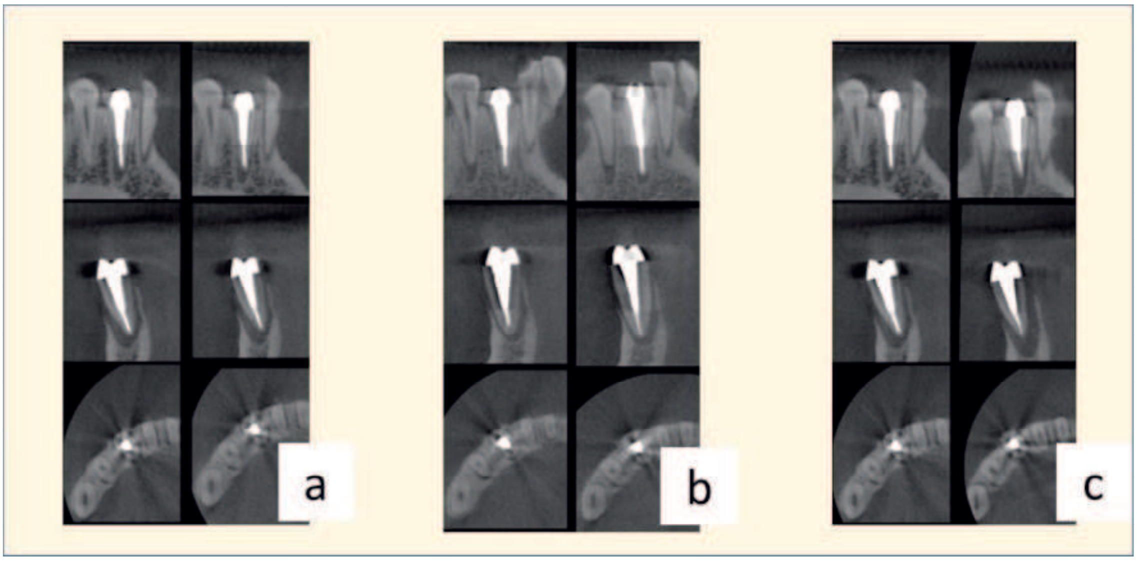

Figure 2. Paired Figures. Parameter (a). Material (b). Oral condition (c).

The observers had to choose which set of images presented higher artifact formation based on the following artifact appearance: hypodense halos, hypodense lines and hyperdense lines. The observers also had to choose which set of images presented higher quality for diagnoses. For all the questions presented the observers could choose between the right set of images, the left set of images or state that there was no difference between both sets of images.

Artifact Quantification

For objective artifact quantification, each DICOM file was read on the scanner's native software (CS3D imaging software, v3.1.9. Carestream Dental Inc., Rochester, USA) and three axial slices of the root were selected and exported as a DICOM image. Datasets in compressed DICOM format were uncompressed with CS3D imaging software tool. The slices represented the post cervical, middle and apical thirds corresponding to the height of the preparation for the metal post (2/3 of the root), being selected at 2, 4 and 6 mm of the cemento-enamel junction, respectively (Figure 3).

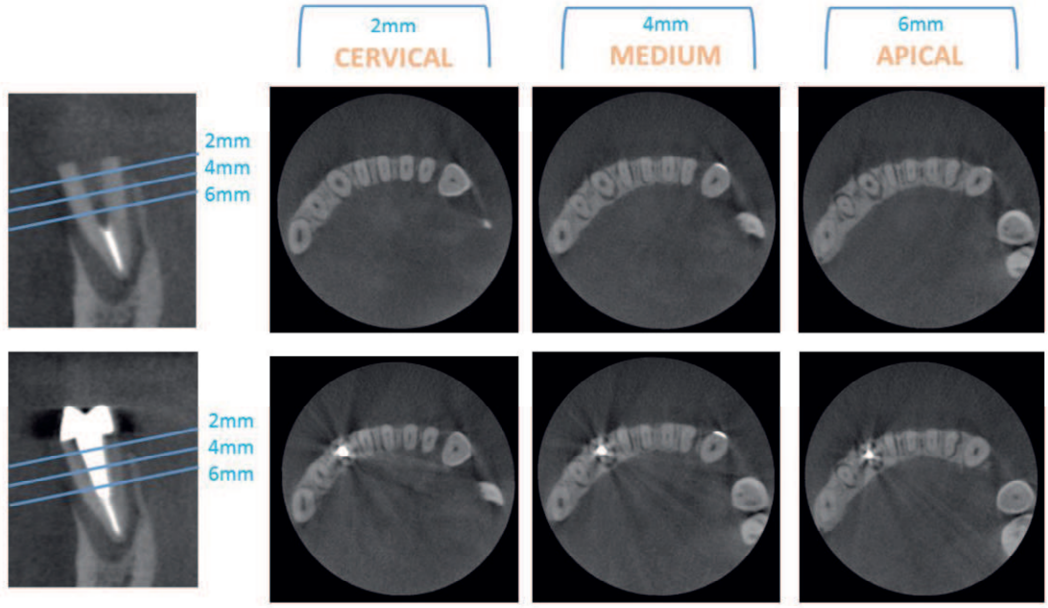

Figure 3. Selected slices (cervical, medium and apical third of the post).

The axial images were imported into the GNU Image Manipulation Program (GIMP) (version 2.8.14, the GIMP Team, USA, available at: http://www.gimp.org/) and the region corresponding to the whole root area was selected with the free selection tool viewed with a zoom of 200x. The resulting images were set to 8-bit scale (256 gray levels), saved with a black background in JPEG format and imported into ImageJ (version 1.48, National Institutes of Health, Bethesda, MD, USA, http:// rsb.info.nih.gov/ij/) (Figure 4).

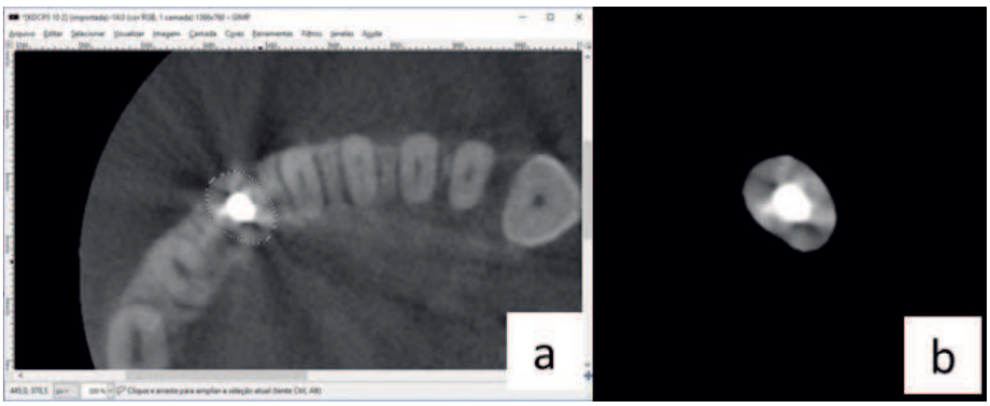

Figure 4. Selecting the root area in the GIMP program (a). Selected area of the root (b).

To remove the area corresponding to the post in the passive fit post images, which did not correspond to the artifact image, an overlap was made between the images of the empty tooth and the tooth with the passively adapted post. This processing was performed in the three-thirds (cervical, middle and apical core) using the imageJ software to acquire a final image of each axial slice.

For image processing, each empty tooth axial image was duplicated, and the threshold tool was applied in order to convert it to a binary image (0 – root canal and background and 255 - dentine). To enable the process, the binary must be zero and 1, 254 values was subtracted. Therefore, the post and background was corresponded to 0 and the dentine to 1. The image subtraction was then processed, which in the program is done using multiplication tool, by subtracting the binary that had the empty conduit and dentin from the image with the post and dentin. As a result, the portion of the image corresponding to the post was excluded from the final image (Figure 5).

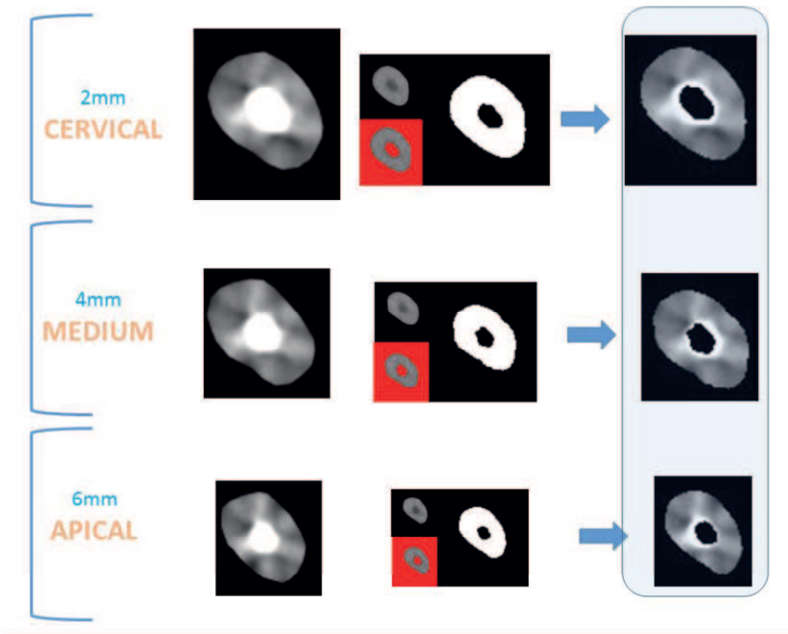

Figure 5. Multiplication between the tooth image with the nucleus and the image of the empty tooth.

Analyzing the dentine area, the threshold tool was used to determine the hypodense and hyperdense artifact areas. In a 8-bit image, with 256 grays levels, the hypodense artifacts range from 9 and to 134, and hyperdense artifacts range from 147 to 255. The remaining tooth (non-affected teeth) was the complementary range between the hypodense and hyperdense artifacts (range from 87 to 207) (Figure 6). Then the percentages of these areas were calculated.

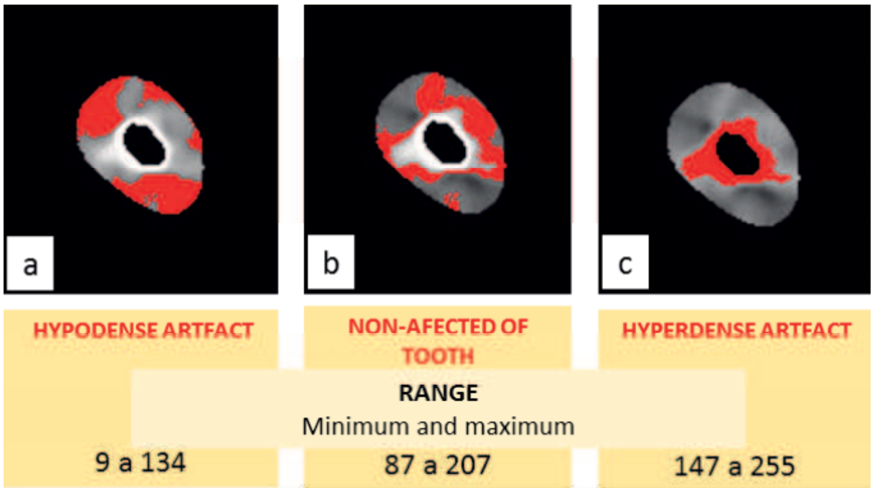

Figure 6. Selecting the area corresponding to the artifacts with the Threshold tool. Hypodense (a). Non-afected of tooth (b). Hyperdense (c).

For objective analysis, 480 evaluations were done (twenty teeth, without and with posts, two different parameters, two different oral conditions, three thirds slices).

Data Analyses

Data were tabulated and statistically analyzed in the Statistical Package for Social Sciences program (SPSS, v. 20, IBM, Chicago, IL). All analyzes were conducted considering the 95% confidence level (α <0.05). Initially, data were assessed for their normality and heterogeneity by means of the Kolmogorov-Smirnov test.

For qualitative artifact volume analysis, data were submitted to Wilcoxon test for statistical comparisons between oral conditions, and Kruskal-Wallis and Mann-Whitney tests for MPs and tube currents (mA). Qui square test was used to determine disagreements between the observers during paired image quality analysis.

For quantitative analysis, 2-way ANOVA was used to evaluate the impact of the studied the independent variables on artifact formation. Post-hoc comparisons were assessed using Tukey test, when the independent variable presented more than 3 groups. To test the hypothesis that the presence of a second non-test tooth in the mandible would increase artifact formation, paired T-test was used.

RESULTS

Volume Qualitative Analysis

For the volume qualitative analysis, double oral condition enhanced hypodense halos for AgPd (Table 1).

Table 1. Statistical comparisons between oral conditions (Wilcoxon test), intracanal filling conditions and CBCT exposure parameters (Kruskal-Wallis and Mann-Whitney tests) for hypodense halos.

Hypodense halos							
Oral condition	**p-value**	**Intracanal condition**	**p-value**	**mA**	Median	Q25-Q75	**p-value**
Simple	0.637	NiCr	0.108	6.3	2.0	1.0-2.0	0.602
				10	2.0	1.0-2.0	
		AgPd		6.3	2.0	2.0-2.0	0.602
				10	2.0	2.0-2.0	
Double		NiCr	0.006	6.3	1.5	1.0-2.0	0.108
				10	2.0	2.0-2.0	
		AgPd		6.3	2.0	2.0-2.0	1.000
				10	2.0	2.0-2.0	

mA= Milliampere; Q25 = Percentile 25%, Q75 = Percentile 75%.

Considering hypodense and hyperdense lines the double oral condition showed more artifacts; and for the double oral condition situation there were statistical differences between intracanal conditions, higher for AgPd (Table 2 and 3).

Table 2. Statistical comparisons between oral conditions (Wilcoxon test), intracanal filling conditions and CBCT exposure parameters (Kruskal-Wallis and Mann-Whitney tests) for hypodense lines.

Hypodense lines							
Oral condition	**p-value**	**Intracanal condition**	**p-value**	**mA**	Median	Q25-Q75	**p-value**
Simple	0.033	NiCr	0.183	6.3	2.0	1.0-2.0	0.183
				10	2.0	2.0-2.0	
		AgPd		6.3	2.0	2.0-2.0	1.000
				10	2.0	2.0-2.0	
Double		NiCr	0.006	6.3	1.5	1.0-2.0	0.799
				10	2.0	1.0-2.0	
		AgPd		6.3	2.0	2.0-2.0	1.000
				10	2.0	2.0-2.0	

mA= Milliampere; Q25 = Percentile 25%, Q75 = Percentile 75%.

Table 3. Statistical comparisons between oral conditions (Wilcoxon test), intracanal filling conditions and CBCT exposure parameters (Kruskal-Wallis and Mann-Whitney tests) for hyperdense lines.

Hyperdense lines							
Oral condition	**p-value**	**Intracanal condition**	**p-value**	**mA**	Median	Q25-Q75	**p-value**
Simple	0.033	NiCr	0.429	6.3	2.0	2.0-2.0	1.000
				10	2.0	2.0-2.0	
		AgPd		6.3	2.0	2.0-2.0	1.000
				10	2.0	2.0-2.0	
Double		NiCr	0.006	6.3	1.5	1.0-2.0	0.108
				10	2.0	2.0-2.0	
		AgPd		6.3	2.0	2.0-2.0	1.000
				10	2.0	2.0-2.0	

mA= Milliampere; Q25 = Percentile 25%, Q75 = Percentile 75%.

For the volume qualitative analysis, there were statistical differences between intracanal conditions and empty tooth ($p<0.001$).

Paired Image Qualitative Analysis

When assessing the paired image quality analysis for exposure parameters (mA), there were only statistical differences between the observers' agreement for the images assessed for diagnostic quality. The paired image quality analysis for intracanal conditions showed no statistical differences between the observers. When evaluating the oral conditions, there were no statistical disagreements between the observers, except for image diagnostic quality (Table 4).

Table 4. Qui-square test of paired image quality evaluation for milliamperage, intracanal conditions and oral co

		Miliamperage (mA)				**Intracanal Condition**				**Oral conditi**	
		Observers				**Observers**				**Observers**	
		1	2	**p-value**		1	2	**p-value**		1	
		N (%)	N (%)			N (%)	N (%)			N (%)	N
Hypodense Halo	**ND**	22(34.4)	20(31.2)	0.565	**ND**	11 (17.2)	9(14.1)	0.315	**ND**	17(26.6)	23(
	6.3	0 (0)	1 (1.6)		**NiCr**	2(3.1)	6(9.4)		**Simple**	6(9,4)	4(
	10	10 (15.6)	11 (17.2)		**AgPd**	19(29.7)	17(26.6)		**Double**	9(14.1)	5(
Hypondese lines	**ND**	21 (32.8)	25 (39.1)	0.266	**ND**	10(15.6)	6(9.4)	0.510	**ND**	18(28.1)	21(
	6.3	0 (0)	0 (0)		**NiCr**	1(1.6)	1(1.6)		**Simple**	1(1.6)	0
	10	11 (17.2)	7 (10.9)		**AgPd**	21(32.8)	25(39.1)		**Double**	13(20.3)	11(
Hyperdense lines	**ND**	21(32.8)	24(37.5)	0.491	**ND**	9(14.1)	9(14.1)	1.000	**ND**	18(28.1)	23(
	6.3	1(1.6)	0 (0)		**NiCr**	1(1.6)	1(1.6)		**Simple**	1(1.6)	1(
	10	10(15.6)	8(12.5)		**AgPd**	22(34.4)	22(34.4)		**Double**	13(20.3)	8(1
Diagnostic Quality	**ND**	5(7.8)	26(40.6)	0.001	**ND**	8(12.5)	11(17.2)	0.287	**ND**	6(9.4)	27(
	6.3	14(21.9)	5(7.8)		**NiCr**	22(34.4)	21(32.8)		**Simple**	22(34.4)	5(
	10	13(20.3)	1(1.6)		**AgPd**	2(3.1)	0(0)		**Double**	4(6.2)	0

mA= Milliampere; ND = No difference.

Artifact Quantitative Analysis

For quantitative image analysis, in simple oral condition, there were no statistical differences between the studied variables for percentage of hypodense artifact. For percentage of non-affected teeth image, there were statistical differences between the cervical axial slice and the apical axial slice for the studied mAs in the presence of both MPs. For percentage of hyperdense artifact, there were statistical differences between apical and cervical thirds axial slices in 6.3 mA for both metal alloys (Table 5).

Table 5. Means and standard deviations of % of hypodense artifact values, % of non-affected teeth image and % of hyperdense artifact values for the studied variables in the simple oral condition.

Exposure parameters		**% of hypodense artifact**			**% of non-affected teeth image**			**% of hyperdense artifact**		
		Alloy	Mean	SD	**Alloy**	Mean	SD	**Alloy**	Mean	SD
6.3	Cervical	NiCr ^{A}	43.4 ^{a}	7.7	NiCr ^{A}	34.3 ^{ab}	6.8	NiCr ^{A}	22.2 ^{b}	4.9
	Medium		42.6 ^{a}	5.0		38.2 ^{bc}	7.6		19.0 ^{ab}	6.2
	Apical		41.7 ^{a}	5.7		42.6 ^{c}	5.0		15.5 ^{a}	3.9
10	Cervical		44.6 ^{a}	4.6		32.3 ^{a}	4.5		23.0 ^{b}	4.7
	Medium		47.1 ^{a}	4.9		32.6 ^{ab}	9.2		20.2 ^{ab}	6.2
	Apical		42.8 ^{a}	2.3		37.8 ^{bc}	8.1		19.3 ^{ab}	7.6
6.3	Cervical	AgPd ^{A}	45.5 ^{a}	3.4	AgPd ^{A}	29.1 ^{ab}	5.4	AgPd ^{B}	25.3 ^{b}	5.3
	Medium		42.6 ^{a}	3.2		35.8 ^{bc}	6.8		21.4 ^{ab}	8.0
	Apical		40.5 ^{a}	3.8		39.7 ^{c}	7.1		19.7 ^{a}	7.0
10	Cervical		44.2 ^{a}	5.1		28.2 ^{a}	6.4		27.5 ^{b}	5.0
	Medium		42.1 ^{a}	4.4		35.2 ^{ab}	6.1		22.5 ^{ab}	6.8
	Apical		43.8 ^{a}	5.1		35.7 ^{bc}	6.2		20.4 ^{ab}	6.4
		p=0.503	p<0.159		p=0.600	p<0.001		p=0.002	p=0.010	

SD = Standard Deviation; Study groups with different superscript letters in the same column indicate statistical differences ($p < 0.05$). Notes: by 2-way ANOVA and post hoc Tukey test.

For the percentage of hypodense artifact, in double oral condition, there were no statistical differences between the studied variables. For percentage of non-affected teeth, there were only statistical differences between the apical and cervical axial slices for 6.3 mA for both metal alloys. For the percentage of hyperdense artifacts, there were statistical differences between the 6.3 mA medium and apical axial slices and 10mA cervical axial slice for both metal alloys (Table 6).

Table 6. Means and standard deviations of % of hypodense artifact values, % of non-affected teeth image and % of hyperdense artifact values for the studied variables in the double oral condition.

Exposure parameters		**% of hypodense artifact**			**% of non-affected teeth image**			**% of hyperdense artifact**		
		Alloy	Mean	SD	**Alloy**	Mean	SD	**Alloy**	Mean	SD
6.3	Cervical	NiCr ^{A}	46.2 ^{a}	2.9	NiCr ^{A}	32.4 ^{a}	6.4	NiCr ^{A}	21.3 ^{ab}	5.7
	Medium		48.0 ^{a}	4.8		33.0 ^{ab}	7.4		18.9 ^{a}	4.7
	Apical		46.1 ^{a}	3.7		36.8 ^{b}	5.1		16.9 ^{a}	4.4
10	Cervical		44.8 ^{a}	3.6		32.1 ^{a}	7.4		22.9 ^{b}	5.3
	Medium		48.5 ^{a}	3.6		32.7 ^{a}	5.9		18.7 ^{ab}	5.2
	Apical		47.0 ^{a}	4.7		34.9 ^{ab}	4.4		18.0 ^{ab}	4.9
6.3	Cervical	AgPd ^{B}	50.6 ^{a}	3.7	AgPd ^{B}	28.3 ^{a}	5.9	AgPd ^{A}	21.0 ^{ab}	5.3
	Medium		51.4 ^{a}	3.4		30.3 ^{ab}	4.4		18.2 ^{a}	5.1
	Apical		47.9 ^{a}	3.8		35.2 ^{b}	4.6		16.8 ^{a}	5.0
10	Cervical		49.1 ^{a}	2.4		25.4 ^{a}	4.9		25.4 ^{b}	6.3
	Medium		50.0 ^{a}	3.8		28.6 ^{a}	4.8		21.3 ^{ab}	7.3
	Apical		48.3 ^{a}	4.7		31.5 ^{ab}	5.0		20.1 ^{ab}	6.8
		p<0.001	p=0.128		p<0.001	p=0.002		p=0.325	p<0.001	

SD = Standard Deviation; Study groups with different superscript letters in the same column indicate statistical differences ($p < 0.05$). Notes: by 2-way ANOVA and post hoc Tukey test.

Comparing single and double oral conditions, the percentage of hypodense artifact was statistically greater for double oral condition (presence of both teste-tooth and nontest tooth). The percentage of non-affected teeth and hyperdense artifacts were greater in the single oral condition (Table 7).

Table 7. Means and standard deviations of simple and double oral conditions for % of hypodense artifact value
image and % of hyperdense artifact values for the studied variables.

Metal alloy	(mA)	Root Thirds	% of hypodense artifact				% of non-affected teeth image				%
			Simple		Double		Simple		Double		S
			Mean	SD	Mean	SD	Mean	SD	Mean	SD	Mea
NiCr	6.3	Cervical	43.4	7.7	46.2	2.9	34.3	6.8	32.4	6.4	22.2
		Medium	42.6	5.0	48.0	4.8	38.2	7.6	33.0	7.4	19.0
		Apical	41.7	5.7	46.1	3.7	42.6	5.0	36.8	5.1	15.5
	10	Cervical	44.6	4.6	44.8	3.6	32.3	4.5	32.1	7.4	23.0
		Medium	47.1	4.9	48.5	3.6	32.6	9.2	32.7	5.9	20.2
		Apical	42.8	2.3	47.0	4.7	37.8	8.1	34.9	4.4	19.3
AgPd	6.3	Cervical	45.5	3.4	50.6	3.7	29.1	5.4	28.3	5.9	25.3
		Medium	42.6	3.2	51.4	3.4	35.8	6.8	30.3	4.4	21.4
		Apical	40.5	3.8	47.9	3.8	39.7	7.1	35.2	4.6	19.7
	10	Cervical	44.2	5.1	49.1	2.4	28.2	6.4	25.4	4.9	27.5
		Medium	42.1	4.4	50.0	3.8	35.2	6.1	28.6	4.8	22.5
		Apical	43.8	5.1	48.3	4.7	35.7	6.2	31.5	5.0	20.4
TOTAL			**43.4**	**4.9**	**48.1**	**4.1**	**35.1**	**7.6**	**31.8**	**6.2**	**21.3**
p-valor (teste t pareado)			**p<0.001**				**p<0.001**				

DISCUSSION

The CBCT scanners provide accurate submillimeter resolution images, allowing 3D reconstruction of the maxillofacial region, providing useful diagnostic imaging. CBCT technology improvements aim to reduce scanning time, improve image fidelity, minimize patient dose,[10,12,13,19,20] and eliminate or at least reduce the large amount of imaging artifacts that may impair diagnostic quality.[2,6,16,17]

Metal restorations, crowns, brackets, metal posts and implants may impair the CT image quality. CT and CBCT images can present a diverse number of artifacts such as beam hardening, scatter, quantum noise (poison noise) and photon starvation, which result in different types of image deterioration, ranging from hyperdense and hypodense lines radiating from the metallic object to darkening of areas in its vicinity and even the complete loss of gray values between adjacent metallic objects.[2]

The darkening area in metal structures vicinity have a negative influence in the diagnostic process, especially root fracture detection, object of several studies.[6,8,9,11,21] The presence of dark streak artifacts mimicking fracture lines, leads to an incorrect diagnosis and treatment planning and follow-up analysis of the region of interest which may not be properly visualized, what in some cases can lead to unnecessary tooth extraction.[6] According to Melo,[21] the presence of an intracanal metal post significantly decreases the detection of artificially created root fractures.

The loss of gray values in tomographic images in the area between adjacent metallic objects is common in clinical practice, because the presence of metals in oral rehabilitation is common and it is usually present in more than one tooth. Therefore, it is important to study the influence of more than one oral metallic object in the amount of artifact formation in CBCT images. Pauwels[2] study showed an increase in the amount of artifacts between metallic structures and stated that, in clinical practice, diagnosis of the area between adjacent metal objects should be avoided, as these regions show excessive loss of the object's projection information. Our results showed that the presence of more than one metal object in the mandible showed an increase of artifact formation, specially hypondense artifacts, both qualitatively and quantitatively and is in agreement with previous studies.[2]

The CBCT scanners allow a large variation of exposure parameters, such as tube current (mA), field of view (FOV), tube voltage (kV), number of basis images and scanner rotation, different sizes and types of detectors, and different reconstruction algorithms that influence the final image quality. These diverse number of exposure parameters have great influence in the generation and, therefore, the amount of radiation which will expose the patient during image acquisition,[2] and may also intensify or minimize the image artifacts.[3,6]

The ALARA principle (as low as reasonably achievable) should always be considered and respected, using the most appropriate acquisition protocol for the specific purpose of the diagnosis.[22] The parameter adjustments must be carefully chosen in order to achieve good quality images for diagnosis purposes with as little radiation exposure as possible.[23,24,25]

The artifact analyzes made in this study, qualitative and quantitative, were chosen so that in a complementary way they could strengthen the answer the study's hypothesis. The qualitative analysis is not concerned with numerical representativeness, but with the deepening of the understanding of the subject in a subjective way, depending on the visual acuity and preference of the observer. In the quantitative analysis, the analyzed data can be quantified, focusing on objectivity, with standardized, neutral instruments and a mathematical language.

A significant dose reduction can be achieved by reducing CBCT tube current (mA) without substantial loss of image quality and without a consistent effect in the artifact areas.[12,26] Lower mAs have been shown to increase image noise; however, the image quality for diagnostic purposes remains acceptable;[27] however, when the mA is reduced to a very low level, 1 mA, a significant reduction in diagnostic accuracy is observed.[13]

In the present study, there was no statistical difference between artifact formation and image quality for diagnosis in the studied mAs on subjective analysis; however, when there was a subtle difference between the parameters, on paired qualitative analysis, the 10 mA images were referred as presenting more artifacts. Our results agree with a previous study, which stated that it is possible to decrease the mA settings to reduce the probability of biological effects due to radiation, without losing diagnostic accuracy.[12]

Although a slight artifact reduction could be observed when increasing different exposure protocols from the same device, the increase in radiation dose is not justified for the sole purpose of metal artifact reduction.[2] An alternative to decrease artifacts without increasing the radiation dose would be choosing a metal alloy that would induce less artifact in the final CT image.

Metal posts were associated with greater artefact formation and compromised the diagnostic performance in previous studies.[12,28] Distinct metal alloys were associated with different amount of artifact formation,[24,25] what indicates that choosing the MP alloy can interfere in the final CBCT image quality. Menezes[11] emphasizes that the presence of metal posts in root canals reduced the sensitivity and accuracy of CT images when detecting root fractures.

In the qualitative analysis of the present study, the difference between the two metal alloys was evidenced only in the double oral condition images for AgPd MPs. This result can be justified by the presence of an extra MP with high atomic number in the mandible which intensified the amount of artifact in the image. In the paired qualitative analysis, were the image was cut to only represent the test-tooth, the AgPd MP presented the worst results in both oral conditions, what indicates that the use of a high atomic number metal alloy can lead to greater diagnosis impairment due to higher artifact formation. The images with a test-tooth and a non-test tooth, although not significant in the paired image analysis, presented more image artifacts, in agreement with the qualitative analysis. The oral conditions studied, single and double, showed that the presence of another metal, even at a distance, may increase the amount of artifact, especially for the hypodense artifacts.

Pauwels[2] when comparing quantitatively exposure protocols of the same device, found that lower and higher mAs did not result in any artefact reduction for some scanners, while other scanners showed a slight artefact reduction for higher mA protocols. This relationship between higher mA and lower artifact quantity agreed with this study's qualitive volume and quantitative analysis; however, in the paired evaluation where subtle differences of artifact quantity were related to higher mA.

The greater preservation of tooth area observed in the apical thirds compared to the cervical thirds can be related to the difference in proportion between the dentin area and the nucleus area; although the total area of the tooth decreases while the nucleus also decreases. The fact that hyperdense artifacts are more evident in the cervical than in the apical third of the teeth; and the apical thirds presented larger non-affected teeth area may indicate that the diagnosis of root fracture in the root apical third can be more accurate than in the cervical thirds.

The quantitative analysis for the material also confirmed the findings of the subjective analysis, where metal alloys with higher atomic numbers attenuate more X-ray and produced a greater amount of artifact. Silver-palladium post (atomic number 47 and 46, respectively) images presented more artifacts than nickel-chromium post (atomic number 28 and 24, respectively) images. Previous studies also confirmed these results, as Panjnoush,[24] when quantifying metal artifacts in CBCT images found that artifacts induced by cobalt-chromium alloys were more severe than those induced by titanium; and Chindasombatjareon[25] found that type IV gold alloy caused the largest artifact areas, followed by cobalt-chromium, titanium and aluminum alloys, respectively. In these studies, the metals or metal alloys with the highest atomic number had the highest amount of artifact.

Therefore, in view of the results found, where the exposure parameters tested do not interfere in the amount of artifact formation, it is recommended to use a lower dose protocol for the patient.

CONCLUSION

The exposure parameters tested did not interfere in the amount of artifact formation, however, the highest atomic number alloy generated a greater amount of image artifact. Hypodense artifacts are more affected by the type and number of metal posts present in the jaws. The presence of another metal, even at a distance, can increase the amount of artifact formation and may impair CBCT diagnostic quality.

REFERENCES

[1] Scarfe WC, Farman AG, Sukovic S. Clinical Applications of Cone-Beam Computed Tomography in Dental Practice. JCDA 2006; 72(1).

[2] Pauwels R, Stamatakis H, Bosmans H et al. Quantification of metal artifacts on cone beam computed tomography images. Clinical Oral Implantology Research 2013; 24: 94-99.

[3] Vasconcelos KF, Nicolielo LFP, Nascimento MC, Haiter-Neto F, Bóscolo FN, Van Dessel J, et al. Artefact expressio associated with several cone-beam computed tomographic machines when imaging root filled teeth. Int Endod Jl 2014; 13.

[4] Beledelli R, Souza, PHC. O que são e como se formam os artefatos nas imagens da tomografia computadorizada de feixe cônico. Revista ABRO 2012; 13(1):2-15.

[5] Schulze R., Heil U, Grob D, Bruellmann DD, Dranischnikow E, Schwanecke U, et al. Artifacts in CBCT: A review. Dentomaxillofacial Radiology 2011; 40:265-273.

[6] Codari M, Vasconcelos KF, Nicolielo LF, Haiter Neto F, Jacobs R. Quantitative evaluation of metal artifacts using different CBCT devices, high-density materials and field of views. Clin Oral Impl Res 2017; 1-6.

[7] Boas FE, Fleischmann D. CT artifacts: Causes and reduction techniques. Imaging Med 2012; 4(2):229-240.

[8] Jakobson SJM, Westphalen VPD, Silva Neto UX, Fariniuk LF, Schroeder AGD, Carneiro E. The influence of metallic posts in the detection of vertical root fractures using different imaging examinations. Dentomaxillofacial Radiology 2014; 43.

[9] Moudi, E, Haghanifar S, Madani Z, Alhavaz A, Bijani A, Bagheri M. Assessment of vertical root fracture using cone-beam computed tomography. Imaging Science in Dentistry 2014; 44:37-41.

[10] Scarfe WC, Farman AG. What is cone-beam CT and how does it work? DentClin. North Am 2008; 52:707-30.

[11] Menezes RF, Araújo NC, Rosa JMCS, Carneiro VSM, Santos Neto AP, Costa V, et al. Detection of vertical root fractures in endodontically treated teeth in the absence and in the presence of metal post by cone-beam computed tomography. BMC Oral Health 2016; 16(48).

[12] Pinto MGO, Rabelo KA, Melo SLS, Campos PSF, Oliveira LSAF, Bento PM et al. Influence of exposure parameters on the detection of simulated root fractures in the presence of various intracanal materials. International Endodontic Journal 2016; 1-9.

[13] Jones D, Mannocci F, Andiappan M, Brown J, Patel S, MClinDent. The effect of alterationof the exposure parameters of a cone-beam computed tomographic scan on the diagnosis of simulated horizontal root fractures. JOE 2015; 41(4):520-525.

[14] Moro M, Agostinho AM, Matsumoto, W. Núcleos metálicos fundidos x pinos pré-fabricados. PCL 2005; 7(36):167-72.

[15] Louro RL, Viera IM, Firme CT. Uso do núcleo metálico fundido na reconstrução de dentes tratados endodonticamente: relato de caso clínico. UFES Rev Odontol 2008; 10(2):69-75.

[16] Benic GI, Sancho-Puchades M, Jung RE, Deyhle H, Hammerle CHF. *In vitro* assessment of artifacts induced by titanium dental implants in cone beam computed tomography. Clin. Oral Impl. Res 2013; 24:378–383.

[17] Likubo, M, Nishioka T, Okura S, Kobayashi K, Sano T, Katsumata A, et al. Influence of voxel size and scan fieldof view on frature-like artefacts from gutta-percha obturated endodontically treated teeth on cone-beam computed tomography images. Oral and maxillofacial radiology 2016; 122(5):631-637.

[18] Schneider SWA comparasion of canal preparations in straight and curved root canals. Oral Surg Oral Med Oral Pathol 1971; 32:271-275.

[19] Ozer, S. Y. Detection of vertical root fractures by using com beam computed tomographywuth variable voxel sizes in a *in vitro* model. JOE 2011; 37(1):75-79.

[20] Jadu FM, Hill ML, Yaffe MJ, Lam EWN. Optimization of exposure parameters for cone beam computed tomography sialography. Dentomaxillofacial Radiology 2011;40:362–368.

[21] Melo SLS, Haiter-Neto F, Correa LR, Scarfe WC, Farman AG. Comparative diagnostic yield of cone beam CT reconstruction using various software programs on the detection of vertical root fractures. Dentomaxillofacial Radiology 2013; 42.

[22] Simões CC, Campos PSF. Influência do tamanho do voxel na qualidade de imagem tomográfica: revisão de literature. RFO 2013; 18(3):361-364.

[23] Katkar R, Steffy DD, Noujeim M, Deahl ST, Geha H. The effect of milliamperage, number of basis images, and export slice thickness on contrast-to-noise ratio and detection of mandibular canal on cone beam computed tomography scans: an in vitro study. Oral and maxillofacial radiology 2016; 122(5):646-653.

[24] Panjnoush M, Kheirandish Y, Kashani PM, Fakhar HB, Youneso F, Mallahi M. Effect of Exposure Parameters on Metal Artifacts in Cone Beam Computed Tomography. J Dent 2016; 13(3):143-150.

[25] Chindasombatjareon J, Kakimoto N, Murakami S, Maeda Y, Furukaw S. Quantitative analysis of metallic artifacts caused by dental metals: comparison of cone-beam and multi-detector row CT scanners. Oral Radiol 2011; 27:114-120.

[26] Sur J, Seki K, Koizumi H, Nakajima K, Okano T. Effects of tube current on cone-beam computerized tomography image quality for presurgical implant planning *in vitro.* Oral Surg Oral Med Oral Pathol Oral Radiol Endod 2010; 110(3):e29-e33.

[27] Pauwels R, Seynaeve L, Henriques JCG, Oliveira Santos C, Souza PC, Westphalen FH, et al. Optimization of dental CBCT exposures through mAs reduction. Dentomaxillofacial Radiology 2015; 44.

[28] Costa FF, Gaia BF, Umetsubo OS, Cavalcanti MGP. Detection of horizontal root fracture wiyh small-volume cone-beam computed tomography in the presence and absence of intracanal metallic post. JOE 2011; 37(10):1456-1459.

5.1 NORMAS DA REVISTA (Dentomaxillofacial Radiology)

Instructions for Authors

TYPES OF PAPERS

Research Articles

Research articles should describe your novel original research in a clear, reproducible way. Research articles should be no more than 7000 words, with generally no more than 50 references.

The abstract for research articles should be constructed under the following subheadings:

- Objectives;
- Methods;
- Results;
- Conclusions;

More information on preparing your submission can be found here.

- You should give sufficient background to your work and the reference list should be representative of the field.
- The method should be described clearly.
- Any limitations of the work should be addressed and discussed.
- The conclusions drawn should be consistent with the results obtained.
- The images included should be clear enough such that the work can be understood.
- Any ethical approval statements should be included where relevant.
- Appropriate statistical analysis of results should be carried out where relevant.

Review Articles and Systematic Reviews

Review articles should provide a broad overview and update on a particular topic, specifically discussing recent research in that area (ca the past 1-3 years). The authors are invited to comment on the state of the field to date and speculate on possible future directions, supported by references.

Review articles should be no larger than 8000 words, typically around 3000 – 6000 words, with 60 – 100 references.

Short Communications

Short communications are brief articles describing original research that is in it's early stages and not ready to be written up as a full paper. This category encompasses work-in-progress etc and typically follows the structure of a research article.

The abstract for short communications papers should be constructed under the following subheadings:

- Objectives;
- Methods;
- Results;
- Conclusions;

More information on preparing your submission can be found here.

Short communications are typically 1000 – 2000 words with 5 – 15 references.

Technical Reports

A technical report is not a hypothesis-driven research report but describes a technique or piece of software of interest to a clinician or researcher in a relevant field of interest.

Technical reports are typically ca. 4000 words with 15 references.

Case Reports

In rare exceptions case reports may be considered for publication in DMFR if they report on very rare cases and are of extraordinary interest for the readership.

The case report should detail the symptoms, observations, diagnosis and treatment, as well as follow-up of a specific patient.

The format for DMFR case reports should be as follows and they should not exceed 2000 words and 15 references.

- Abstract
- Introduction
- Case Report
- Discussion.

Letters to the Editor

Letters to the Editor should comment on an article that has appeared in a previous issue of DMFR. These will be forwarded to the authors of that article to allow them to reply. If accepted, the letters will be published together.

- Correspondence should not, unless absolutely necessary, contain tables or figures.
- All authors to a letter must sign it.
- No more than six key references should be included.

PREPARING YOUR SUBMISSION

For guidelines regarding word count, figure/table count and references for all DMFR article types see here.

Authors' names and affiliations should not appear anywhere on the manuscript pages or the images (to ensure blind peer-review).

Teeth should be designated in the text using the full English terminology. In tables and figures individual teeth can be identified using the FDI two-digit system, i.e. tooth 13 is the first permanent canine in the right maxilla region.

- Author contribution statement
- Title page
- Abstract
- Main text
- References
- Tables
- Figures
- Appendices
- Supplementary material
- Units, symbols and statistics

AUTHOR CONTRIBUTION STATEMENT

DMFR requires that an author contribution statement accompany each submission, outlining the contributions of each author towards the work. A template statement can be downloaded here.

DMFR requires that for all submitted papers:

- All the authors have made substantive contributions to the article and assume full responsibility for its content; and
- All those who have made substantive contributions to the article have been named as authors.

The International Committee of Medical Journal Editors recommends the following definition for an author of a work, which we ask our authors to adhere to:

Authorship be based on the following 4 criteria [1]:

- Substantial contributions to the conception or design of the work; or the acquisition, analysis, or interpretation of data for the work; AND
- Drafting the work or revising it critically for important intellectual content; AND
- Final approval of the version to be published; AND
- Agreement to be accountable for all aspects of the work in ensuring that questions related to the accuracy or integrity of any part of the work are appropriately investigated and resolved.

1 The International Committee of Medical Journal Editors, Roles and Responsibilities of Authors, Contributors, Reviewers, Editors, Publishers, and Owners: Defining the Role of Authors and Contributors, http://www.icmje.org/roles_a.html

TITLE PAGE

The title page is a separate submission item to the main manuscript and should provide the following information:

- Title of the paper. Abbreviations other than CT or MRI should not be used in the title.
- A shortened version of the title (no more than 70 characters in length, including spaces) should be provided for use as the running head. Abbreviations are permissible.
- Type of Manuscript (see all types of manuscript)
- Author names should appear **in full** (in the format: "first name, initial(s), last name), qualifications and affiliations.
- Statement indicating any source of funding or financial interest where relevant should be included.
- A cover letter or statement can be included into the title page, but please note this is not a compulsory item.

Blind title page

A blind title page should be included with the full manuscript, giving only the title (i.e. without the authors’ names and affiliations), for use in the peer-review process.

ABSTRACT

The abstract should be an accurate and succinct summary of the paper, not exceeding **250 words**. For papers containing research: the abstract should be constructed under the following subheadings:

- Objectives;
- Methods;
- Results;
- Conclusions.

These subheadings should appear in the text of the abstract and the abstract should not contain references. The abstract should: indicate the specific objective or purpose of the article; describe the methods used to achieve the objective, stating what was done and how it was done; present the findings of the methods described – key statistics should be included; present the conclusion of the study based solely on the data provided, and highlight the novelty of the work.

Beneath the abstract please select up to 5 keywords from the current Medical Subject Headings (MeSH).

MAIN TEXT

Please organise your paper in a logical structure with clear subheadings to indicate relevant sections. It is up to the authors to decide the specific nature of any subheadings as they see fit. Research papers typically follow the structure:

- Introductory section;
- Methods and materials/patients;
- Results;
- Discussion;
- Conclusion;
- Acknowledgments (if relevant).

Present results in a clear logical sequence. The conclusions drawn should be supported by the results obtained and the discussion section should comment critically on the findings and conclusions as well as any limitations of the work.

Acknowledgments should be brief and should indicate any potential conflicts of interest and sources of financial support.

An appendix may be used for mathematical formulae or method details of interest to readers with specialist knowledge of the area.

In addition:

- Avoid repetition between sections.
- Avoid repetition of text featured in tables and the main body of the article.
- Abbreviations and acronyms may be used where appropriate, but must always be defined where first used.
- The names and locations (town, country) of manufacturers of all equipment and non-generic drugs must be given.
- Avoid the use of footnotes.
- Use SI units throughout the text (Grays, Sieverts not RADs and REMs).

REFERENCES

- Authors are responsible for the accuracy of the references. Only papers closely related to the work should be cited; exhaustive lists should be avoided. All references must appear both in the text and the reference list.
- References should follow the Vancouver format.
- In the text, references are cited in numerical order as superscript numbers starting at 1. The superscript numbers are placed AFTER the full point.
- At the end of the paper they should be listed (double-spaced) in numerical order corresponding to the order of citation in the text.
- A reference cited in a table or figure caption counts as being cited where the table or figure is first mentioned in the text.
- Papers in press may be included in the list of references.
- Do not include references to uncompleted work or work that has not yet been accepted for publication. Abstracts and/or papers presented at meetings not in the public domain should not be included as references.
- References to private communications should be given only in the text (i.e. no number allocated). The author and year should be provided.
- If there are 6 or fewer authors, list them all. If there are 7 or more, list the first 6 followed by et al.
- Abbreviations for titles of medical periodicals should conform to those used in the latest edition of Index Medicus.
- The first and last page numbers for each reference should be provided.
- Abstracts and letters must be identified as such.

Examples of references:

Journal article:
Gardner DG, Kessler HP, Morency R, Schaffner DL. The glandular odontogenic cyst: an apparent entity. J Oral Pathol 1988; 17:359–366.

Journal article, in press:
Dufoo S, Maupome G, Diez-de-Bonilla J. Caries experience in a selected patient population in Mexico City. Community Dent Oral Epidemiol (in press).

Complete book:
Kramer IRH, Pindborg JJ, Shear M. Histological typing of odontogenic tumours (2nd edn). Berlin: Springer Verlag, 1992.

Chapter in book:
DelBalso AM, Ellis GE, Hartman KS, Langlais RP. Diagnostic imaging of the salivary glands and periglandular regions. In: DelBaso AM (ed). Maxillofacial imaging. Philadelphia, PA: WB Saunders, 1990, pp 409–510.

Abstract:
Mileman PA, Espelid I. Radiographic treatment decisions - a comparison between Dutch and Norwegian practitioners. J Dent Res 1986; 65: 609 (Abstr 32).

Letter to the Editor:
Gomez RS, de Oliveira JR, Castro WH. Spontaneous regression of a paradental cyst. Dentomaxillofac Radiol 2001; 30: 296 (letter).

Journal article on the internet:
Abood S. Quality improvement initiative in nursing homes: the ANA acts in an advisory role. Am J Nurs [serial on the Internet]. 2002 Jun [cited 2002 Aug 12];102(6):[about 3 p.]. Available from: http://www.nursingworld.org/AJN/2002/june/Wawatch.htm.

Homepage/Web site:
Cancer-Pain.org [homepage on the Internet]. New York: Association of Cancer Online Resources, Inc.; c2000-01 [updated 2002 May 16; cited 2002 Jul 9]. Available from: http://www.cancer-pain.org/.

TABLES

Tables should be referred to specifically in the text of the paper but provided as separate files.

- Number tables consecutively with Arabic numerals (1, 2, 3, etc.), in the order in which they appear in the text.
- Give each table a short descriptive title.
- Make tables self-explanatory and do not duplicate data given in the text or figures.

- Aim for maximum clarity when arranging data in tables. Where practicable, confine entries in tables to one line (row) in the table, e.g. "value (±sd) (range)" on a single line is preferred to stacking each entry on three separate lines.
- Ensure that all columns and rows are properly aligned.
- Include horizontal rules at the top and bottom of a table and one below the column headings. If a column heading encompasses two or more subheadings, then the main headings and subheadings should be separated by a single short rule. No other rules should be included, neither horizontal nor vertical.
- Appropriate space should be used to separate columns. Rows should be double-spaced.
- A table may have footnotes if necessary. These should be referred to within the table by superscript letters, which will then also be given at the beginning of the relevant footnote. Begin each footnote on a new line. A general footnote referring to the whole table does not require a superscript letter.
- Define abbreviations in tables in the footnotes even if defined in the text or a previous table.
- Submit tables as editable text.

FIGURES

Figures should be referred to specifically in the text of the paper.

- Number figures consecutively using Arabic numerals (1, 2, 3, etc.) and any figure that has multiple parts should be labelled alphabetically (e.g. 2a, 2b).
- Concise, numbered legend(s) should be listed on a separate sheet. Avoid repeating material from the text.
- Abbreviations used in figures should be defined in the caption.
- Labelling of artwork should be Arial 8 point font.
- Ideally, figure sizes should be 84 mm wide, 175 mm wide or the intermediate width of 130 mm.

Files

- Supply image files in EPS, TIFF, PDF or JPEG format.
- TIFF is preferred for halftones, i.e. medical images such as radiographs, MR scans etc.
- EPS is preferred for drawn artwork (line drawings and graphs).
- For JPEG files, it is essential to save at maximum quality, i.e. "10", to ensure that quality is satisfactory when the files are eventually decompressed.

- Files supplied in Word, PowerPoint or Excel may prove acceptable, but please supply in EPS, TIFF or JPEG if practicable. Other formats will not be usable.
- Do not supply GIF files – GIF is a compressed format that can cause quality problems when printed.
- Upload each figure separately and numbered.

Colour

- Unless essential to the content of the article, all illustrations should be supplied in black and white with no colour (RGB, CMYK or Pantone references) contained within them.
- The cost of reproduction of colour images will be charged to the author at the following rates: £300 for one colour image, £500 for two colour images and £100 for each subsequent additional colour image. All prices are exclusive of UK VAT.
- Images that do need to be reproduced in colour should be saved in CMYK, with no RGB or Pantone references contained within them.

Resolution

- Files should be saved at the appropriate dpi (dots per inch) for the type of graphic (the typical screen value of 72 dpi will not yield satisfactory printed results). Lower resolutions will not be usable.
- Line drawings – save at 800 dpi (or 1200 dpi for fine line work).
- Halftone and colour work – save at 300 dpi.

Composition

- The image should be cropped to show just the relevant area (i.e. no more than is necessary to illustrate the points made by the author whilst retaining sufficient anatomical landmarks). The amount of white space around the illustration should be kept to a minimum.
- Supply illustrations at the size they are to be printed, usually 76 mm wide (single column of text) or for especially large figures 161 mm (two columns of text).
- Annotations, e.g. arrows, should be used to indicate subtle but salient points. All annotations should be included within the images supplied.
- Patient identification must be obscured.

Additional points to note:

- Do not put a box around graphs, diagrams or other artwork.

- Avoid background gridlines unless these are essential (e.g. confidence limits).
- Fonts should be Adobe Type 1 standard – Helvetica or Times are preferred.
- Ensure that lettering is appropriately sized – should correspond to 8 or 9 pt when printed.
- Include all units of measurement on axes.
- All lines (e.g. graph axes) should have a minimum width of ¼ pt (0.1 mm) otherwise they will not print; 1 pt weight is preferable.
- Avoid using tints (solid black and white or variations of crosshatching are preferred), but any tints that are used must be at a minimum 5% level to print (but do not use too high a tint as it may print too dark).
- Do not use three-dimensional histograms when the addition of a third dimension gives no further information.

APPENDICES

Appendices should be used to include detailed background material that is essential for the understanding of the manuscript e.g. statistical analyses, very detailed preliminary studies, but which is too comprehensive to include as part of the main text.

Where possible, authors are encouraged to include all relevant material in the main body of the text, however, if an appendix is necessary it should be supplied as a separate file. If more than one appendix is included, these should be identified using different letters.

- An appendix may contain references, but these should be listed separately and numbered A1, A2, etc.
- Appendices must be referred to in the main text in the relevant section.

SUPLEMENTARY MATERIAL

Supplemental material is intended for material that would add value to your manuscript but is not essential to the understanding of the work. Supplementary material is typically used for including material that can not be accommodated in print form, for example multimedia files such as dynamic images, video/audio files etc.

There are no restrictions on supplementary file formats, though it is recommended that authors choose file types that the majority of readers will be able to open e.g.

- Text/Data: PDF, Word, Excel, Powerpoint, .txt
- Graphics: TIF, PNG, JPEG, GIF
- Video: AVI, MOV, MP4, MPEG, WMV
- Audio: mp3, m4a

UNITS, SYMBOLS AND STATISTICS

Authors should use the International System of Units (SI) [1]. Units of radiation should be given in SI, e.g. 1 Sv, 1 Gy, 1 MBq. Exceptions are mmHg for blood pressure and g dl–1 for haemoglobin. For guidance, authors can refer to the publication Units, Symbols and Abbreviations. A guide for medical and scientific authors [2].

- All radiation factors (dose/time/fractionation) must be listed.
- Equations should be numbered (1), (2) etc. to the right of the equation. Do not use punctuation after equations.
- Do not include dots to signify multiplication – parameters should simply be typed closed up, or with a multiplication sign if necessary to avoid ambiguity.

Statistical Guidelines

The aim of the study should be clearly described and a suitable design, incorporating an appropriate number of subjects, should be used to accomplish the aim. It is frequently beneficial to consult a professional statistician before undertaking a study to confirm it has adequate power, and presentation of a power calculation within the paper demonstrates the ability of the study to detect clinically or biologically meaningful effects.
Details should be provided on selection criteria, whether data were collected prospectively or retrospectively, and any exclusions or losses to follow-up that might affect the study population. Information on subject characteristics in groups being compared should be given for any factors that could potentially bias the comparison of the groups; such information is often best presented in a tabular format in which the groups are in adjacent columns. If the study was randomized, details of the randomization procedure should be included.
Measures of variation should be included for all important results. When means are presented, the standard deviation or the standard error of the mean should also be given, and it should be clear which of these two measures is being quoted. When medians are given, measures of variation such as the interquartile range or overall range should also be included. Estimates of differences, e.g. between two means being compared, should be provided with 95% confidence limits to aid the reader and author to interpret the results correctly. Note that estimation of the size of effects, e.g. treatment or prognostic factor effects, is as important as hypothesis testing. Statistical procedures should be described and referenced for all p-values given, and the values from which they were derived should be included. The validity of statistical procedures should

also be confirmed, e.g. the t-test requires normal distribution(s) in the basic data and the chi-squared test is not valid when the expected numbers in cells are less than 5. Data may sometimes be transformed, e.g. using a log or square root transformation, to achieve normality. Non-parametric tests should be used when the conditions for normality are not met. It should be noted, however, that the Wilcoxon signed rank test (the non-parametric equivalent of the paired t-test) is semi-quantitative. If more than two groups are being compared then an analysis of variance should be performed before undertaking comparisons of pairs of groups. You are advised to seek the help of a professional statistician if you are uncertain of the appropriateness or interpretation of statistical methods.

Analysis of repeated measurements on the same subject can give rise to spurious results if comparisons are made at a large number of different time points. It is frequently preferable to represent each subject's outcome by a single summary measure chosen for its appropriateness. Examples of such measures are the area under the curve, the overall mean, the maximum or minimum, and the time to reach a given value. Simple statistics can then be applied to these summary measures.

The results of the evaluation of a test procedure should state clearly the criteria used to define positivity, and the sensitivity, specificity, positive predictive value and negative predictive value should all be quoted together with their 95% confidence limits.

1. Goldman DT, Bell RJ, eds. The International System of Units (SI). 5th edn. London, UK: HMSO; 1987.

2. Baron DN, ed. Units, symbols and abbreviations. A guide for medical and scientific authors. 5th edn. London, UK: Royal Society of Medicine Press; 1994.

PUBLISHING ETHICS

The BIR's publishing ethics are in place to promote ethical publication practice across all our books, journals and any other publications. This page outlines our policies on the major ethical principles of academic publishing. The BIR is a member of COPE (Committee On Publication Ethics).

- Authorship
- Original data
- Declaration of funding source and conflicts of interest
- Author misconduct and article withdrawal
- Studies involving human and animal subjects

- Informed consent

AUTHORSHIP

To be listed as an author, an individual should have made substantial contributions to all four categories established by the International Committee of Medical Journal Editors (ICMJE):

- "Substantial contributions to the conception or design of the work; or the acquisition, analysis, or interpretation of data for the work"; AND
- "Drafting the work or revising it critically for important intellectual content"; AND
- "Final approval of the version to be published"; AND
- "Agreement to be accountable for all aspects of the work in ensuring that questions related to the accuracy or integrity of any part of the work are appropriately investigated and resolved".

The ICMJE further states that "Acquisition of funding, the collection of data, or general supervision of the research group, by themselves, do not justify authorship." The BIR asks that authors fulfill the ICMJE requirements to be so listed.

On submitting an article our authors must agree to the terms and conditions of our Licence to Publish which warrants that 'all the Authors have made substantive contributions to the Article and assume full responsibility for its content.'

Individuals who have not made substantial contributions in all three categories but who have made substantial contributions either to some of them or in other areas should be listed in the Acknowledgments.

Changing the list of authors

Once a manuscript has been received by the BIR, any changes in authorship will necessitate additional information:

Adding an author

The addition of an author requires that a 'confirmation of author status - addition' letter be signed and submitted to the editorial office by all authors, indicating agreement with both the addition and the placement of the proposed author in the listing of authors. The author's contribution information should also be provided.

Removing an author

The deletion of an author requires that a 'confirmation of author status - removal' letter be signed and submitted to the editorial office by all authors, **including the one being removed**, indicating agreement with both the removal of the relevant author.

If the removed author is to be added to the Acknowledgments section, receipt of a signed 'confirmation of author status - removal' letter will be taken that all named authors agree to the same.

ORIGINAL DATA

The Editors reserve the right to ask to inspect the raw data on which the results of a submitted article are based.

DECLARATION OF FUNDING SOURCE AND CONFLICTS OF INTEREST

Source of funding

We ask that authors always make clear the source of any funding for research work or towards publication of their article. This applies to all article types and all sources of funding, including government, private or commercial sources as well as funding towards publication support for an article such as funding towards our article processing charge for BIR|Open, colour charges or editorial assistance.

Conflicts of interest

Conflicts of interest are defined as those that, through their potential influence on behaviour or content or from perception of such potential influences, could undermine the objectivity, integrity or perceived value of publication.

We ask that the authors declare fully any conflicts of interest in their manuscript. A conflict of interest is an interest of the author(s) which may influence the objectivity, integrity and value of the publication.

Examples include:

- Employment by any organisation with a financial interest in or financial conflict with the publication of the article.

- Funding source – financial support by any organisation with a financial interest in or financial conflict with the publication of the article.
- Personal financial interests – financial interests such as stocks and shares in companies with a financial interest in or financial conflict with the publication of the article; consultation fees or other remuneration from organisations with a financial interest in or financial conflict with the publication of the article; patents or patent applications which may be affected by publication of the article.
- Membership to organisations with a financial interest in or financial conflict with the publication of the article.

If a reviewer or editor of a paper feels a conflict of interest in making a decision on a paper, the paper should be returned to the editorial office for transfer to another editor/reviewer.

AUTHOR MISCONDUCT AND ARTICLE WITHDRAWAL

Author misconduct

Author misconduct includes:

- fabrication or falsification of research results
- plagiarism
- submission of your manuscript to more than one journal at the same time
- redundant publications.

The BIR endorses the policies of the International Committee of Medical Journal Editors and is a member of CrossCheck – the plagiarism detection initiative. All published articles have been screened using plagiarism detection software.

Article withdrawal

Very occasionally circumstances may arise where an article published in BJR is affected by one of the issues above or may contain inaccurate data and must be withdrawn, retracted, removed or replaced. More detail on each of these processes is outlined below:

Article withdrawal:

This process is used for Advance articles – these are post-peer review versions of articles that have not yet undergone full copyediting and typesetting. These can occasionally contain errors, be submitted more than once in error or infringe our publishing ethics.

Article retraction:

Infringements of our publishing ethics as detailed above OR errors in submission/publication in a published, final version of an article will result in the article being retracted. A retraction notice written by the authors and or editors/editorial office detailing the reason for retraction will be published in a subsequent issue of the journal, with a link on the electronic version to the original version of the article.

Article removal:

Very rarely an article may need to be removed, such as in cases where the article poses a serious health risk, is defamatory, infringes on the legal rights of others or is the subject of a court order.

Article replacement:

This occurs where false or inaccurate data in the original article – which may pose a health risk – is replaced.

STUDIES INVOLVING HUMAN AND ANIMAL SUBJECTS

Humans

Research on human subjects submitted to BIR journals must have been carried out in accordance with the standards set out in the Code of Ethics of the World Medical Association (Declaration of Helsinki) for experiments involving humans.

Authors should include a statement at the end of the manuscript clarifying that:

- such standards have been adhered to;
- the research procedures were approved by the responsible committee on human or animal experimentation (institutional or regional); and
- that informed consent was obtained for experimentation with human subjects.

N.B. Please note, if your research involves human subjects who may be identifiable from the images, data or details included in your paper you will need to obtain informed consent for publication. Read more about informed consent for publication here.

Please ensure that all patient details are anonymised as much as possible in your manuscript before submitting, this includes images, names, initials, hospital numbers etc.

Animals

Research on animal subjects submitted to BIR Journals must have been carried out in accordance with:

- the UK Animals (Scientific Procedures) Act, 1986 and associated guidelines; OR
- the EU Directive 2010/63/EU for animal experiments; OR
- the latest edition of the National Institutes of Health guide for the care and use of Laboratory animals.
-

Authors should include a statement at the end of the manuscript clarifying that:

- such standards have been adhered to; and
- the research procedures were approved by the responsible committee on human or animal experimentation (institutional or regional).

We encourage the use of and adherence to the ARRIVE guidelines when writing and submitting your animal research to BIR Journals authors may find the ARRIVE checklist useful when submitting.

INFORMED CONSENT

Authors should make all efforts to anonymise/emilinate patient data/images/identifying details from their manuscript. Please refer to our informed consent policy for for more detail.

If there is any possibility that the patient can be identified in an illustration, photograph or other image, written informed consent for these details of the case to be published (incl. images, case history and data) must be obtained from the patient or a parent/guardian as appropriate and a line stating that this has been received must be included in the manuscript.

The BIR endorses the International Committee of Medical Journal Editors' policy on informed consent.

The informed consent of all patients participating in reported trials for their case to be published (incl. images, case history and data) must be obtained and a statement to this effect must be included in submitted manuscripts, when relevant.

For case reports and case reviews

All case-based articles in *BJR|case reports* and *DMFR* require informed consent from the patient or guardian/relative where the patient is unable to give consent. Please refer to our informed consent policy for more detail.

INFORMED CONSENT

The BIR journals *BJR|case reports* and *DMFR* accept submissions of case reports. *BJR|case reports* also accepts submissions of case reviews

All case-based articles published in BIR journals:

- should be sufficiently anonymised so as to protect patient identity; AND
- require informed consent for the case to be published (incl. images, case history and data) from the patient or guardian/relative where the patient is unable to give consent.

Technical notes focusing on a specific patient('s) case and/or containing identifying information will also require informed consent for the case to be published (incl. images, case history and data) from the patient or guardian/relative where the patient is unable to give consent.

N.B. informed consent to publish is not the same as informed consent to treat

Obtaining informed consent from the patient to publish their case (incl. images, case history and data) is a vital aspect of writing, submitting and publishing your case report (or case review). This is separate from any informed consent to treat you may have obtained from the patient (or family/guardian) to perform a specific treatment/investigation/medical procedure as part of their care.

Obtaining informed consent to publish a case will involve clearly communicating with the patient (or family/guardian) your intention to write up their clinical case (incl. images, case history and data) for publication in an open access medical journal and ensuring they understand the implications of this.

We ask that you obtain written informed consent to publish; you do not need to submit this with your manuscript but we reserve the right to request a copy if necessary.

BEFORE SUBMITTING

You must have signed informed consent ***for the case to be published*** (incl. images, case history and data) from the patient(s)/patient's guardian/relative before submitting to a BIR Journal.

If the patient is deceased or non-contactable:

Authors must make extensive efforts to seek informed consent from the next of kin (guardian/relative).

WHEN PREPARING YOUR MANUSCRIPT

Please ensure all patient data is anonymised as much as possible, e.g. obscure identifying features in photographs, patient/hospital numbers in medical images, omit information such as occupation, location, personal circumstance etc. which is unnecessary for interpretation of the case.

It should be stated clearly in the manuscript that informed consent ***for the case to be published*** (incl. images, case history and data) was obtained.

You are not required to upload the consent documentation when submitting, however, we may request copies of the documentation at any time.

Example statement:

"Written informed consent for the case to be published (incl. images, case history and data) was obtained from the patient(s) for publication of this case report, including accompanying images".

PEER-REVIEW PROCESS

DMFR is committed to publishing high quality content and our peer-review process plays a key role in assessing and improving submitted papers.

All papers submitted to DMFR undergo peer review. Upon submission papers are initially assessed by a member of our editorial board for scientific validity and relevance to the DMFR readership. Papers which are suitable for peer review are then sent for review to two independent reviewers.

Our peer-review process is double-blind to ensure unbiased reports and we aim to provide all our authors with constructive, helpful feedback.

Once all reports have been received the editor makes a decision on the paper which is then communicated to the author.

Manuscripts requiring revisions will be reassessed by the handling editor upon resubmission and may be subject to further review dependent on the extent of revisions required.

Our average submission to first decision time is 2 weeks.

COPYRIGHT, LICENCES AND PERMISSIONS

Please find information below on reusing content in BIR Publications and reusing content previously published in BIR Publications, as well as your rights and options as an author.

If you can't find the answer to your query here please contact publications@bir.org.uk.

PERMISSION TO REUSE PREVIOUSLY PUBLISHED CONTENT...

… in your article for a BIR Publications journal

If you are including a figure, chart, table or other material in your BIR Publications journal article that has been previously published, you must obtain permission to reproduce that content (usually from the publisher) prior to publication. Please note that the payment of any fees required by the previous publisher is the responsibility of the author

For figures/charts/tables/other materials that have been previously published in a journal or book permission can often be obtained from the copyright clearance centre. If you can not find the relevant publication there, it is best to contact the publisher of the original work.

Please note:

- If your article is being published in BJR and DMFR, these titles are available in print as well as online so you will need permission to reproduce the requested content in electronic and print format.
- If your article is being published in BJR|case reports this title is online only so you will need permission to reproduce the requested content in electronic format only.

Any reproduced material must be **clearly labelled** as being reproduced from elsewhere and the original source adequately referenced.

All content marked as reproduced in your manuscript will be raised by our production department at typesetting and proof reading stages (subject to acceptance) and you should be able to provide proof of permission to reproduce this content (in print and online) from the relevant rights holder.

… from an article in a BIR Publications jornal

BJR, BJR|case reports, DMFR, Imaging, BIR Books and Supplements

The BIR holds the copyright or the exclusive right to publish original content featured in BJR, BJR|case reports, DMFR, Imaging and other BIR Publications such as books and supplements. To request permission or reuse materials from these titles, please access the Copyright Clearance Centre and search for the content you wish to reuse. You can also use the ‘Get Permissions’ link on the right hand navigation bar next to the article you wish to reuse content from.

BJR|case reports and BIR|Open articles in BJR and DMFR

BJR|case reports is an open access title and all content is published under a CC BY 4.0 licence. This licence allows others to reuse, distribute, change and build upon work or sections of work featured in BJR|case reports, even for commercial gain as long as the original work is credited.

BIR|Open articles in BJR and DMFR can be published under two different types of licence:

- Creative commons attribution (CC BY) licence; or
- Creative commons attribution non-commercial licence (CC BY NC)

For more information about the specific licence that applies to the work in question and the associated rights, please see the final version of the article hosted on our website for the licence details.

If you wish to reuse content from an open access BJR or DMFR article and have any further questions, please contact publications@bir.org.uk.

YOUR RIGHTS AS NA AUTHOR:

BJR and DMFR

All articles currently published in BJR and DMFR are published under the terms of our Licence to Publish. This means our authors retain copyright in their work, are free to make copies of the final published version for their own personal use and can re-use individual figures, tables and continuous sections of the text (under 350 words) in other publications by a third party, with proper attribution of the original work, without having to seek permission or pay a fee to the BIR.

Authors are also permitted to archive their work in accordance to our archive policy.

Imaging, BIR Books and Supplements

All articles currently published in Imaging, BIR Books and Supplements are subject to bespoke Licence to Publish agreements. For more information about your rights as an author please consult your Licence to Publish or contact us on publications@bir.org.uk.

BJR|case reports and BIR|Open articles in BJR and DMFR

- **BJR|case reports**

  BJR|case reports is an open access title and all content is published under a CC BY 4.0 licence. This licence allows reuse, distribution, changes and building upon the work

POST ACCEPTANCE

Publish ahead of print

The version of your paper accepted by us will be published online under DMFR Papers in Press. The article will not yet have undergone the post-acceptance production process, namely, copy-editing, typesetting. It will citable as soon as it appears online. When your article is published in its final version in an issue, the BJR Papers in Press version of your article will be removed.

Proofs

The corresponding author will receive a typeset proofs of their paper as a PDF file by email approximately 1 week after acceptance. You will be asked to read the proof carefully and answer any queries raised by the production process.

e-Prints and reprints

We will provide 35 free electronic reprints of each published paper to be distribute as the authors wish. These reprints are available as PDF downloads. When the issue is published online, the corresponding author will be notified.

Additional reprints may be ordered using the form accompanying the proofs.

Continuous publication

DMFR moved to continuous publication in 2013. Continuous publication is article-based publishing as opposed to issue-based publishing. When an article is in its final form, rather than waiting for the article to be in a print issue before it is technically published, the article is published in its final form online. The Version of Record will be the online article and accepted articles are cited using a volume and article identifier rather than a traditional issue and page number, please see below for example.

Articles should be cited in the following format:

Schilling J, Gomes LCR, Benavides E, Nguyen T, Paniagua B, Styner M, et al. Regional 3D superimposition to assess temporomandibular joint condylar morphology. Dentomaxillofac Radiol 2014; 43: 20130273.

The benefit to authors is that acceptance to publication time will be reduced and there is no more waiting for the article to appear in a finalised issue before it is technically published. This modern publishing model will allow our titles to achieve an even faster 'Speed to Publication', benefitting our authors and readers in disseminating the latest in research as soon as possible.

INFORMATION FOR NIH-FUNDED AUTHORS

Your paper has been accepted for publication in *BJR* or *DMFR*

All articles are uploaded to PubMed Central by BIR Publications in their final published version. Open access articles appear in full after publication, and all other articles are embargoed for 12 months with only the title, author details and abstract appearing in that time, which falls within the time frame specified by NIH funding policy. It is the author's responsibility to track and link the paper through Submission Method A.

...and you have opted for open access publication in *BJR* or *DMFR*

Thank you for deciding to publish your article on an open access basis. Open access articles are uploaded in full in their final published version to PubMed Central by BIR Publications. It is the responsibility of the author to deposit the final peer-reviewed manuscript into the NIH Manuscript Submission system (NIHMS). The submission is through Method C. Instructions can be found here and here.

Your paper has been accepted for publication in *BJR|case reports*

All articles in *BJR|case reports* are published on an open access basis under a CC BY licence. It is the responsibility of the author to deposit the final peer-reviewed manuscript into the NIH Manuscript Submission system (NIHMS). The submission is through Method C. Instructions can be found here and here.

PROMOTING YOUR ARTICLE

We want to make sure all the effort and expertise of our authors is read by the widest possible audience. BIR Journals works hard to promote your content through e-alerts, our enhanced journal-hosting platform, search engine optimisation (SEO), conference attendance, marketing, social media campaigns and more.

As an author you can get involved and help disseminate your work to a wide network of your peers.

While writing your paper...

While you're writing take a moment to consider your readers - what words and key phrases would they enter in to a search engine to find articles on the topic you're writing on?

- Choose a clear, descriptive title. Search engines weight the words in your title most heavily in determining what your article is about, so make sure anyone reading it would get a good idea of the article content from your title.
- Use key words and phrases consistently throughout your article. The more these appear in the abstract and text, the more likely your article is to be returned high up in the results list of a search for those words/phrases (and related ones).

A word of caution, while it's prudent to think about how someone might search on the topic of your article, and how to maximise the chances of them finding your article, don't let that get in the way of your writing style and make your work repetitive.

6 CONSIDERAÇÕES FINAIS

A partir da análise dos resultados encontrados, pode-se concluir que:

- Os núcleos de NiCr e AgPd formam halos hipodensos, linhas hipodensas e hiperdensas. Os artefatos hipodensos ocupam áreas maiores que os hiperdensos;
- Os parâmetros de exposição testados não interferem na quantidade de formação de artefatos para o tomógrafo Carestream;
- Ligas de números atômicos superiores geram maior quantidade de artefatos;
- A presença de outro metal nos maxilares pode aumentar a quantidade artefatos de imagem e pode prejudicar o diagnóstico por imagem de TCFC;
- De forma geral, o terço cervical apresenta maior quantidade de artefato hiperdenso comparado ao apical.

REFERÊNCIAS

ANUSAVICE, K. J. **Phillips, materiais dentários**. 11 ed. Rio de Janeiro: Elsevier, 2005.

BARRET, J. F.; KEAT, N. Artifacts in CT: recognition and avoidance. **RadioGraphics**, v. 24, n. 6, p. 1679-1691, nov./dec. 2004.

BELEDELLI, R.; SOUZA, P. H. C. O que são e como se formam os artefatos nas imagens da tomografia computadorizada de feixe cônico. **Revista ABRO**, v. 13, n. 1, p. 2-15, jan./jun., 2012.

BENIC, G. I. et al. In vitro assessment of artifacts induced by titanium dental implants in cone beam computed tomography. **Clin. Oral Impl. Res**. v. 24, p. 378–383, 2013.

BOAS, F. E.; FLEISCHMANN, D. CT artifacts: Causes and reduction techniques. **Imaging Med**, v. 4, n. 2, p. 229-240, 2012.

BRASIL. Conselho Nacional de Saúde. Resolução 466, de 12 de dezembro de 2012. Regulamenta os aspectos éticos em pesquisas envolvendo seres humanos. Disponível em: http://conselho.saude.gov.br/resolucoes/2012/Reso466.pdf.

CHINDASOMBATJAREON, J. et al. Quantitative analysis of metallic artifacts caused by dental metals: comparison of cone-beam and multi-detector row CT scanners. **Oral Radiol.,** v. 27, p. 114-120, 2011.

CODARI, M. et al. Quantitative evaluation of metal artifacts using different CBCT devices, high-density materials and field of views. **Clin Oral Impl Res**, p. 1-6, 2017.

COSTA, F. F. et al. Detection of horizontal root fracture wiyh small-volume cone-beam computed tomography in the presence and absence of intracanal metallic post. **JOE,** v. 37, n. 10, p. 1456-1459, oct. 2011.

GARIB, D. G. et al. Tomografia computadorizada de feixe cônico (Cone beam): entendendo este novo método de diagnóstico por imagem com promissora aplicabilidade na Ortodontia. **R Dental Press Ortodon Ortop Facial**, Maringá, v. 12, n. 2, p. 139-156, mar./abr., 2007.

JADU, F. M. et al. Optimization of exposure parameters for cone beam computed tomography sialography. **Dentomaxillofacial Radiology**, v. 40, p. 362–368, 2011.

JAKOBSON, S. J. M. et al. The influence of metallic posts in the detection of vertical root fractures using different imaging examinations. **Dentomaxillofacial Radiology**, v. 43, 2014.

JONES, D. et al. The effect of alterationof the exposure parameters of a cone-beam computed tomographic scan on the diagnosis of simulated horizontal root fractures. **JOE**, v. 41, n. 4, p. 520-525, abril 2015.

KAMBUROGLU, K. Use of dentomaxillofacial cone beam computed tomography in dentistry. **World J Radiol,** v. 7, n. 6, p. 128-130, jun. 2015.

KATKAR, R. et al. The effect of milliamperage, number of basis images, and export slice thickness on contrast-to-noise ratio and detection of mandibular canal on cone beam computed tomography scans: an in vitro study. **Oral and maxillofacial radiology**, v. 122, n. 5, p. 646-653, nov. 2016.

KUTEKEN et al. Artefato metálico em tomografia computadorizada de feixe cônico**. Rev. Odontol. Univ. Cid. São Paulo**, v. 27, n. 3, p. 220-228, set./dez. 2015.

LIKUBO, M. et al. Influence of voxel size and scan fieldof view on frature-like artefacts from gutta-percha obturated endodontically treated teeth on cone-beam computed tomography images. **Oral and maxillofacial radiology,** v. 122, n. 5, p. 631-637, nov. 2016.

LOURO, R. L.; VIERA, I. M.; FIRME, C. T. Uso do núcleo metálico fundido na reconstrução de dentes tratados endodonticamente: relato de caso clínico. **UFES Rev Odontol**, v. 10, n. 2, p. 69-75, 2008.

McCABE, J. F.; WALLS, A. W. G. **Materiais dentários diretos**. 8 ed. São Paulo: Santos, 2006.

MELO, S. L. S. et al. Comparative diagnostic yield of cone beam CT reconstruction using various software programs on the detection of vertical root fractures. **Dentomaxillofacial Radiology**, v. 42, 2013.

MENEZES, R. F. et al. Detection of vertical root fractures in endodontically treated teeth in the absence and in the presence of metal post by cone-beam computed tomography. **BMC Oral Health,** v. 16, 48, 2016.

MORO, M.; AGOSTINHO, A. M.; MATSUMOTO, W. Núcleos metálicos fundidos x pinos pré-fabricados. **PCL**, v. 7, n. 36, p. 167-72, 2005.

MORTMAN, R. E. Technologic Advances in Endodontics. **Dent Clin**, v. 55, p. 461–480, 2011.

MOUDI, E. et al. Assessment of vertical root fracture using cone-beam computed tomography. **Imaging Science in Dentistry**, v. 44, p. 37-41, 2014.

NOORT, R. V. **Introdução aos materiais dentários**. 2 ed. Porto Alegra: Artmed, 2004.

OZER, S. Y. Detection of vertical root fractures by using com beam computed tomographywuth variable voxel sizes in a *in vitro* model. **JOE,** v. 37, n. 1, p. 75-79, jan. 2011.

PANJNOUSH, M. et al. 2016. Effect of Exposure Parameters on Metal Artifacts in Cone Beam Computed Tomography. **J Dent**, v. 13, n. 3, p. 143-150, June 2016.

PAUWELS, R. et al. Quantification of metal artifacts on cone beam computed tomography images. **Clin. Oral Impl**, v. 24, p. 94-99, 2013.

PAUWELS, R. et al., 2015. Optimization of dental CBCT exposures through mAs reduction. **Dentomaxillofacial Radiology**, v. 44, 2015.

PINTO, M. G. O. et al. Influence of exposure parameters on the detection of simulated root fractures in the presence of various intracanal materials. **International Endodontic Journal,** p. 1-9, abril 2016.

VASCONCELOS, K. F. et al. Artefact expressio associated with several cone-beam computed tomographic machines when imaging root filled teeth. **Int Endod Jl**, v. 13, 2014.

SCARFE, W. C.; FARMAN, A. G.; SUKOVIC, S. Clinical Applications of Cone-Beam Computed Tomography in Dental Practice, **JCDA**, v. 72, n. 1, feb. 2006.

SCARFE, W. C.; FARMAN, A. G. What is cone-beam CT and how does it work? **DentClin. North Am**, v. 52, p. 707-30, 2008.

SCHNEIDER, S. W. A comparasion of canal preparations in straight and curved root canals. **Oral Surg Oral Med Oral Pathol,** v. 32, p. 271-275, 1971.

SCHULZE, R. et al. Artifacts in CBCT: A review. **Dentomaxillofacial Radiology,** v. 40, p. 265-273, 2011.

SIMÕES, C. C.; CAMPOS, P. S. F. Influência do tamanho do voxel na qualidade de imagem tomográfica: revisão de literature. **RFO**, v. 18, n. 3, p. 361-364, set./dez. 2013.

SUR, J. et al. Effects of tube current on cone-beam computerized tomography image quality for presurgical implant planning *in vitro.* **Oral Surg Oral Med Oral Pathol Oral Radiol Endod,** v. 110, n.3, p. e29-e33, 2010.

WHITE, S. C.; PHAROAH, M. J. P. **Oral Radiology: Principles and Interpretation**. 7 ed. Elsevier Health Sciences, 2014. 679p.

ANEXOS

ANEXO A


FOLHA DE ROSTO PARA PESQUISA ENVOLVENDO SERES HUMANOS

PESQUISADOR RESPONSÁVEL

INSTITUIÇÃO PROPONENTE

PATROCINADOR PRINCIPAL

ANEXO B

UNIVERSIDADE ESTADUAL DA PARAÍBA
PRÓ-REITORIA DE PÓS-GRADUAÇÃO E PESQUISADOR
COMITÊ DE ÉTICA EM PESQUISA ENVOLVENDO SERES HUMANOS
COMISSÃO NACIONAL DE ÉTICA EM PESQUISA ENVOLVENDO SERES HUMANOS
PLATAFORMA BRASIL

Relator: 08.
Pesquisador Responsável: Ana Priscila Lira de Farias Freitas
CAAE: 60637616.6.0000.5187
Data da relatoria: 15/12/2016
SITUAÇÃO DO PROJETO: APROVADO
Apresentação do Projeto: Projeto intitulado " AVALAIAÇÃO DOS ARTEFATOS FORMADOS PR NÚCLEOS METÁLICOS FUNDIDOS: MICRO TC X TCFC", encaminhado para análise, ao Comitê de Ética em Pesquisa da Universidade Estadual da Paraíba, com fins à obtenção de parecer favorável ao início das atividades propostas, as quais resultarão em Trabalho de Conclusão de Curso de Pós-Graduação em Odontologia, da Universidade Estadual da Paraíba – Campus I.
Objetivo Geral da Pesquisa: Avaliar os artefatos formados por núcleos metálicos fundidos por meio de Micro TC e da TCFC
Avaliação dos Riscos e Benefícios: Considerando a justificativa e os aportes teóricos e metodologia apresentados no presente projeto, e ainda considerando a relevância do estudo as quais são explícitas suas possíveis contribuições, percebe-se que a mesma não trará riscos aos participantes da pesquisa.
Comentários e Considerações sobre a Pesquisa: A presente proposta de estudo é de suma importância quanto papel e atribuições das Instituições de Ensino Superior (IES), estando dentro do perfil das pesquisas de construção do ensino-aprendizagem significativa, perfilando a formação profissional baseada na tríade conhecimento-habilidade-competência, preconizada pelo MEC. Portanto, tem retorno social, caráter de pesquisa científica e, contribuição na formação de profissionais da área de saúde. O projeto encontra-se completo, sem pendências.
Considerações sobre os Termos de apresentação obrigatória: Ao analisar os documentos necessários para a integração do protocolo científico, encontramos todos os documentos necessários e obrigatórios. Estando tais documentos em harmonia com as exigências preconizadas pela Resolução 466/12/CNS/MS.
Recomendações: Os tópicos do projeto encontram-se bem articulados, havendo toda uma harmonia entre eles.
Conclusões ou Pendências e Lista de Inadequações: O projeto atende as exigências protocolares. Diante do exposto, somos pela aprovação. Salvo melhor juízo.

ANEXO C

UEPB

UNIVERSIDADE ESTADUAL DA PARAÍBA
CEP — COMITÊ DE ÉTICA EM PESQUISA
R. Baraúnas, 351 - Universitário, Campina Grande – PB
CEP: 58429-500
(083) 3315-3300

TERMO DE DOAÇÃO DE DENTES

Ao Comitê de Ética em Pesquisa da UNIVERSIDADE ESTADUAL DA PARAÍBA

Declaro que doei 20 (vinte) pré-molares inferiores aos pesquisador(es) Daniela Pita de Melo, Ana Marly Araújo Maia e Ana Priscila Lira de Farias Freitas a fim de viabilizar a execução da pesquisa intitulado "AVALIAÇÃO DOS ARTEFATOS FORMADOS POR NÚCLEOS METÁLICOS FUNDIDOS: MICRO TC X TCFC." Igualmente declaro que estes dentes foram extraídos previamente ao conhecimento da pesquisa supracitada, por indicação clínica e independentemente da mesma, sendo armazenado em frasco único, o que impossibilita a identificação dos indivíduos dos quais os dentes foram extraídos.

Campina Grande, 10 de Agosto de 2016.

Heitor Silva Borges

Heitor Silva Borges CPF: 040.583.963-31
CRO: 5744 PB
Rua Emiliano Rosendo da Silva, 75 – Novo Bodocongó. Bloco K, Apto 1102
TEL.: 083-99653 5552

ANEXO D

UEPB

UNIVERSIDADE ESTADUAL DA PARAÍBA
CAMPUS VIII – PROFª. MARIA DA PENHA
CENTRO DE CIÊNCIAS, TECNOLOGIA E SAÚDE

DECLARAÇÃO

Para os fins que forem necessários a Direção do Centro de Ciências, Tecnologia e Saúde – CCTS da UEPB informa que a profa. **Ana Marly Maia** foi autorizada para retirar do Laboratório de Morfologia do Curso de Odontologia do Campus VIII/UEPB peças anatômicas (ossos do crânio e face) para fins de pesquisa no Programa de Pós-Graduação em Odontologia da UEPB/Campus I.

Araruna - PB, 31 de outubro de 2016

Atenciosamente

Manuel Antonio Gordón Núñez
Diretor do Centro de Ciências, Tecnologia e Saúde
Universidade estadual da Paraíba
Matr. 825584-6

ANEXO E

Avaliação Subjetiva – Presença de Artefato

Avaliador:____Data____________

- O software do sistema Kodak 9000 permite a visualização dos cortes tomográficos em 3 planos distintos, demonstrados no esquema que pode ser visualizado no quadrante superior direito da tela. Cada cor representa um plano: Laranja-axial, rosa-sagital e verde-coronal.
- No quadrante superior esquerdo podemos observar o plano axial, no quadrante inferior esquerdo o plano sagital e no quadrante inferior direito o plano coronal.
- Utilizando as linhas guias para cada plano, pode-se percorrer as unidades dentárias em qualquer sentido.
- A presença de artefato deve ser avaliada em todo o volume adquirido – todos os cortes.
- Os artefatos metálicos foram subdivididos nos 3 tipos: halo hiperdensos, linhas hipodensas e linhas hipodensas.
- **Em caso de dúvida, não hesite em perguntar.**

PASTA ______________________

Volume_____1_____	**Halo Hipodenso**	**Linhas Hipodensas**	**Linhas Hiperdensas**
Ausência			
Presença moderada			
Presença severa			

Volume_____2_____	**Halo Hipodenso**	**Linhas Hipodensas**	**Linhas Hiperdensas**
Ausência			
Presença moderada			
Presença severa			

Volume_____3_____	**Halo Hipodenso**	**Linhas Hipodensas**	**Linhas Hiperdensas**
Ausência			
Presença moderada			
Presença severa			

Volume_____4_____	**Halo Hipodenso**	**Linhas Hipodensas**	**Linhas Hiperdensas**
Ausência			
Presença moderada			
Presença severa			

ANEXO F

Avaliação Subjetiva – Presença de Artefato – IMAGENS PAREADAS

Avaliador:____Data____________

- A imagem foi exportada no formato Tiff;
- As imagens estão dispostas em pares e com três cortes para cada amostra (coronal, sagital e axial);
- A presença de artefato deve ser avaliada comparativamente entre a amostra da esquerda e da direita;
- Os artefatos metálicos foram subdivididos nos 3 tipos: halo hiperdenso, linhas hipodensas e linhas hipodensas. Deve-se escolher qual imagem apresenta maior quantidade de artefato para cada tipo dos mesmos;
- Deve-se escolher qual das imagens apresenta maior qualidade para diagnóstico de fratura radicular;
- **Em caso de dúvida, não hesite em perguntar.**

PASTA ______________________

Figura 1

Qual das imagens apresenta maior quantidade de artefato:

Halo hipodenso:	Esquerda ( )	Não há diferença ( )	Direita ( )
Linhas hipodensas:	Esquerda ( )	Não há diferença ( )	Direita ( )
Linhas hiperdensas:	Esquerda ( )	Não há diferença ( )	Direita ( )

Qual das imagens apresenta maior qualidade para diagnóstico de fratura radicular?

Esquerda ( ) Não há diferença ( ) Direita ( )

Figura 2

Qual das imagens apresenta maior quantidade de artefato:

Halo hipodenso:	Esquerda ( )	Não há diferença ( )	Direita ( )
Linhas hipodensas:	Esquerda ( )	Não há diferença ( )	Direita ( )
Linhas hiperdensas:	Esquerda ( )	Não há diferença ( )	Direita ( )

Qual das imagens apresenta maior qualidade para diagnóstico de fratura radicular?

Esquerda ( ) Não há diferença ( ) Direita ( )

APÊNDICE A

UNIVERSIDADE ESTADUAL DA PARAÍBA
CEP — COMITÊ DE ÉTICA EM PESQUISA
R. Baraúnas, 351 - Universitário, Campina Grande – PB.
CEP: 58429-500.
(083) 3315-3300

TERMO DE CONSENTIMENTO LIVRE E ESCLARECIDO

Uma vez que não é possível identificar os indivíduos doadores dos dentes, sujeitos da pesquisa, não será aplicado o termo de consentimento livre e esclarecido (TCLE) aos voluntários da pesquisa intitulada" AVALIAÇÃO DOS ARTEFATOS FORMADOS POR NÚCLEOS METÁLICOS FUNDIDOS: MICRO TC X TCFC.", sob a responsabilidade do(s) pesquisador(es) Ana Priscila Lira de Farias Freitas, Profª Drª Daniela Pita de Melo e Prof. Drª. Ana Marly Araújo Maia.